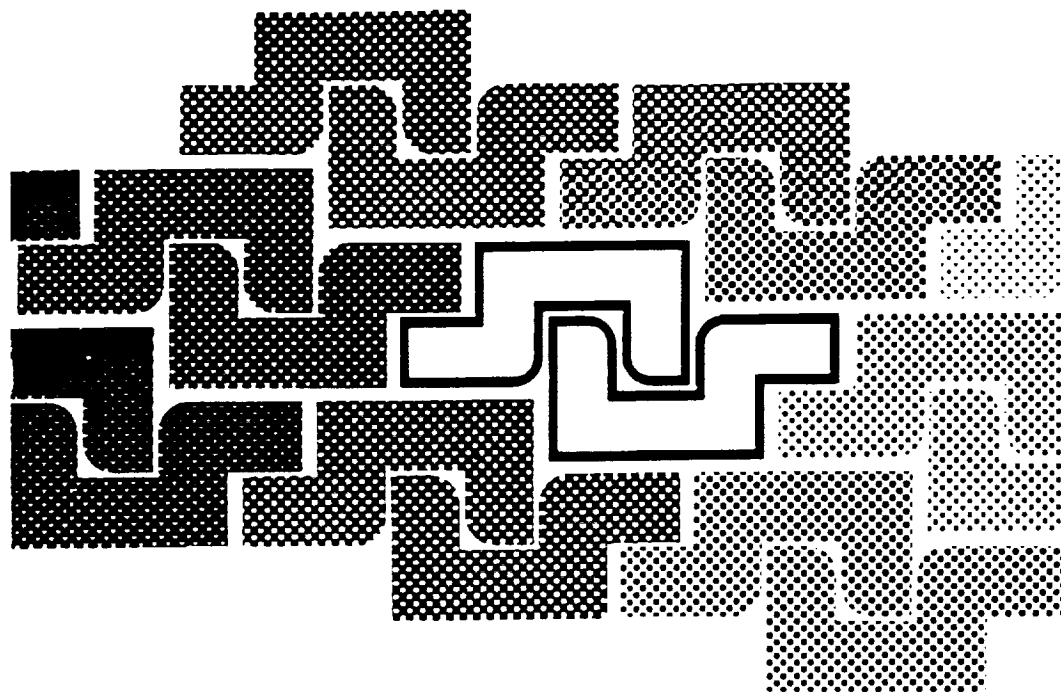APPENDIX W

N95- 25934

Terrestrial Space Radiation and Its Biological Effects

Edited by

Percival D. McCormack
Charles E. Swenberg and
Horst Bücker

NATO ASI Series

1988

(278)

SPACE RADIATION DOSIMETRY ON U.S.
AND SOVIET MANNED MISSIONS

E. V. Benton
University of San Francisco

T. A. Parnell
NASA-Marshall Space Flight Center

SPACE RADIATION DOSIMETRY ON U.S. AND SOVIET MANNED MISSIONS[1]

E. V. Benton* and T. A. Parnell**

*Department of Physics, University of San Francisco
Ignatian Heights, San Francisco, CA 94117, U.S.A.
**NASA Marshall Space Flight Center, Huntsville, AL
35812, U.S.A.

ABSTRACT

Radiation measurements obtained on board U.S. and Soviet spacecraft are presented and discussed. A considerable amount of data has now been collected and analyzed from measurements with a variety of detector types in low-Earth orbit. The objectives of these measurements have been to investigate the dose and LET spectra within the complex shielding of large spacecraft. The shielding modifies the external radiation (trapped protons, electrons, cosmic ray nuclei) which, in turn, is quite dependent on orbital parameters (altitude, inclination). For manned flights, these measurements provide a crew exposure record and a data base for future spacecraft design and flight planning. For the scientific community they provide useful information for planning and analyzing data from experiments with high sensitivity to radiation. In this paper, results of measurements by both passive and active detectors are described. High-LET spectra measurements were obtained by means of plastic nuclear track detectors (PNTDs) while thermoluminescent dosimeters (TLDs) measured the dose. A few flights carried active detectors—tissue equivalent ion chambers (TEICs), particle spectrometers (generally to measure the LET distribution), and particle rate counters. On some flights, thermal and epithermal neutrons were measured with the use of fission foils, and metal samples analyzed by gamma ray spectroscopy measured low levels of several activation lines. PNTDs consisting of different combinations of CR-39, polycarbonate, and cellulose-nitrate sheets have proved to be an effective means of measuring the high-LET spectra. To date, they have been used on all the Space Shuttle flights including Spacelabs 1 and 2,

and the earlier missions of the Gemini, Apollo and Skylab series. The assembly of various types of detectors, especially the large numbers deployed in the crew compartments, modules, access tunnels, and pallets of Spacelabs 1 and 2, have provided the most comprehensive mapping yet available of the radiation environment of a large spacecraft in low Earth orbit. They demonstrate the efficiency and advantages of coordinated measurements with passive and active detectors. The dosimetric results accumulated for over twenty-five years indicate the difficulty of accurately predicting the total picture of radiation phenomena as it will be encountered by space station crews and other future missions. Understanding the effects of different types and configurations of shielding is also of particular importance. Detailed results of the measurements and comparison with calculated values are described.

1.0 INTRODUCTION

Exposure to ionizing radiation of space crews engaged in long-term space missions such as space stations, moon bases and trips to Mars, poses a set of complex scientific and technological problems which need to be resolved before adequate radiation protection can be achieved. Areas of immediate interest include providing adequate radiation measurements (i.e., dosimetry) and understanding the complex radiation environment and the effects of shielding on the different components of the incoming radiations. This paper summarizes the results of radiation dosimetry measurements which have been performed in the last twenty-five years in the U.S. and Soviet space flight programs.

The complex radiation environment and special conditions involved in space flight pose unique problems in the dosimetry of high energy radiation. First of all, there are a number of primary sources of radiation including galactic cosmic rays, radiation trapped by the Earth's geomagnetic field, rare but sometimes intense solar flares and, potentially, that from nuclear on-board sources. These radiations have broad energy spectra and may contain a variety of charged particle types such as protons, electrons, alpha particles and photons, as well as heavier nuclei including those of the entire periodic table. A gamut of secondary radiations includes mesons, neutrons, recoiling nuclei; also bremsstrahlung, π^0 decay, and activation photons. These radiations have a spatial and temporal variation which can result in orders of magnitude changes of radiation levels inside spacecraft. For low-Earth orbit the fluxes and energy spectra are dependent on altitude,

orbit inclination, solar conditions, position, and spacecraft orientation in orbit, and the amount, type and placement of shielding materials in the spacecraft. Since the equipment and supplies are usually unevenly distributed throughout the spacecraft, different radiation levels are found in the different portions of the spacecraft, as well as uneven radiation of various parts of the astronauts' bodies. The degree of non-uniformity depends upon the penetrating ability of radiation and can result in steep gradients of absorbed dose within the body. Finally, while some secondary radiation is less penetrating, in certain circumstances secondary radiations may have even greater penetrability than the primary; for example, in the situation involving the attenuation of low-energy electrons by the skin of the spacecraft and subsequent production of penetrating bremsstrahlung radiations /Parnell et al., 1986; Benton, 1986/.

2.0 DOSE AND DOSE-RATE (Mostly Passive Detectors)

For the past twenty-five years, a variety of spacecraft have been developed and used by the U.S. and U.S.S.R. In order to present an idea of the shielding involved, Fig. 1 shows (roughly to scale) the three earliest Soviet spacecraft, namely Vostok, Voskhod and Soyuz, and one of the latest space-station types of spacecraft, the Salyut-7, which is shown not to scale.

The weight and dimensions of the early spacecraft (not including antennas, solar cell banks, or panels) are (1) Vostok: about 10,400 lbs., 8.7 feet in diameter, 23.8 feet in length; the manned capsule is 7.5 feet in diameter; (2) Voskhod: about 12,000 lbs., 9.0 feet in diameter, 34.5 feet in length; the manned capsule is 7.5 feet in diameter; (3) Soyuz: 11.4 feet in diameter; the aft interstage is 14.8 feet in diameter; the length is 40.2 feet with a manned capsule 10.3 feet in diameter /Janni, 1969a/. The Salyut-7 section shown is about 15 meters in length, excluding the transport ships and a new module which was added later. With the addition of the new module and a Soyuz P-14 manned transport, the Salyut complex stretches for some 115 feet and has a mass of approximately 103,000 lbs.; it also includes a Gemini spacecraft-sized re-entry vehicle. Clearly, the size, mass and therefore the effective shielding within the different spacecraft vary greatly. While knowledge of the exact shielding is always somewhat poor, for the pre-Salyut flights the shielding (arithmetic average) generally exceeded 17 g/cm^2 /Petrov et al., 1975/.

2.1 Soviet Measurements

In Table 1 is shown some of the dosimetry data from Soviet spacecraft for the time period 1960-1983 /Petrov et al., 1975; Akatov et al., 1984; Markelov and Chernykh, 1982/. Most of the average dose-rate data is in the
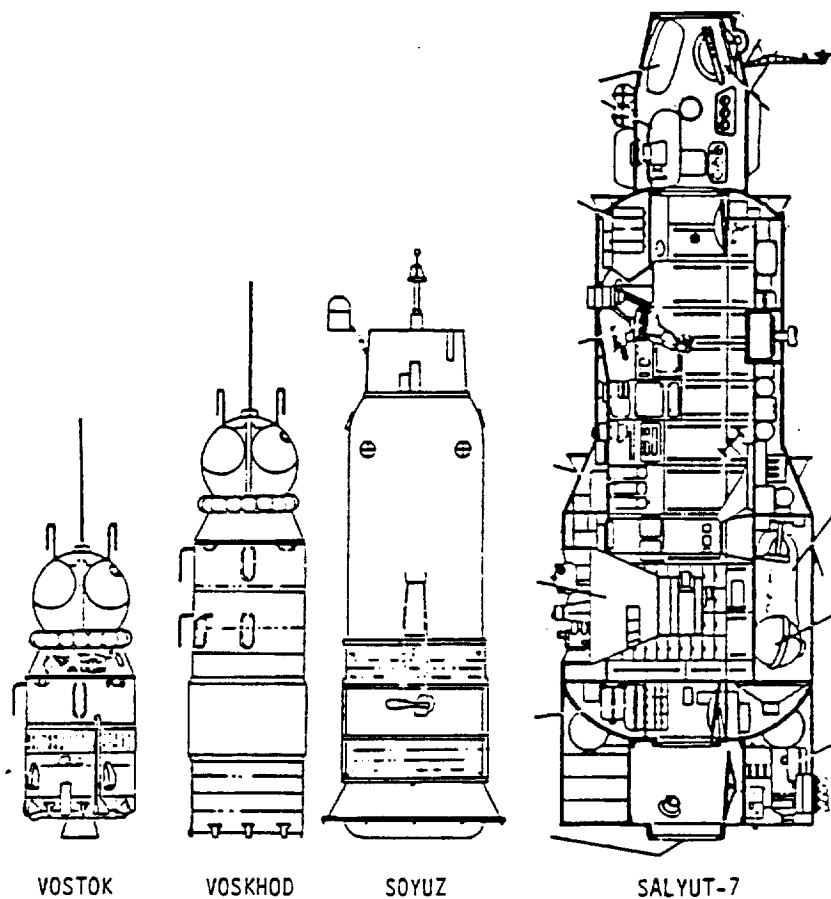
VOSTOK   VOSKHOD   SOYUZ   SALYUT-7

Fig. 1. Four types of Soviet manned spacecraft /Janni, 1969/.
(Salyut not drawn to scale with other three.)

range of 10-30 mrad/day and reflects the fact that the Soviet manned space-
craft have consistently flown in fairly low-altitude orbits. The main excep-
tion to that was the 1965 flight with an apogee of 500 km which recorded a
higher dose of 65 mrads per day, still well below that which has been recor-
ded on a number of U.S. flights. The measurements in Table 1 were performed
with a variety of active and passive types of devices, with the early mea-
surements being accurate to about +/- 15 percent. From these early measure-
ments, the Soviets concluded that they had observed dependence of dose-rate
on the period of solar activity, noting that "during the 1964 solar minimum
the dose-rates increased by roughly a factor of two." Also, "increasing the
shielding from 2 to 15 g/cm^2 did not greatly decrease the dose-rate"/Petrov
et al., 1975/. This again is partially a consequence of the low altitude
(see Section 3.1).

732

Table 1. Dosimetry Data from Soviet Spacecraft

Date		Orbital Parameters			Average Dose Rate (mrad/day)
month	year	inclination	apogee (km)		
08*	1960	65°	340		12.5
04	1961	65°	330		7.2
08	1961	65°	240		8.4
05	1962	65°	330		16.0
08	1962	65°	370		45.0
08	1962	65°	240		13.5
10	1962	65°	350		30.0
11	1962	65°	380		30.0
12	1962	65°	400		35.0
04	1963	65°	340		18.0
05	1963	65°	370		15.0
05	1963	65°	400		30.0
06	1963	65°	300		12.0
06	1963	65°	220		15.5
06	1963	65°	230		15.5
10	1964	65°	410		29.0
04	1965	65°	500		65.0
09	1965	65°	360		16.0
10	1965	65°	340		15.0
11	1965	65°	350		18.0
03	1966	65°	310		11.0
04	1966	65°	330		15.5
07	1966	73°	350		21.0
07	1966	52°	360		26.0
08	1966	65°	360		29.0
11	1966	65°	340		22.0
12	1966	65°	320		14.0
11	1968	52°	∿210		21.2
01	1969	52°	∿210		20.0
01	1969	52°	∿210		24.0
10	1969	52°	∿210		14.0
10	1969	52°	∿210		13.0
10	1969	52°	∿210		14.0
06	1970	52°	∿210		13.0
12	1973	52°	∿210		12.5
07**	1974	51.6°	270	Salyut-3	15
12	1974	51.6°	270	Salyut-4	13
06	1976	51.6°	260	Salyut-5	15
09	1977	51.6°	275	Salyut-6	16
05-06+	1980	---	---	Salyut-6	10.0
03-07	1983	51.6°	340	Salyut-7	16.7
07-08	1983	51.6°	340	Salyut-7	14.8
08-09	1983	51.6°	340	Salyut-7	18.0
09-11	1983	51.6°	492	Salyut-7	16.0

*Petrov et al., 1975
**Akatov et al., 1984
+Markelov and Chernykh, 1982

In Table 2 are listed the absorbed and equivalent radiation doses for the crews of Salyut 3-6 spacecraft, while Table 3 lists the doses incurred by members of the international crews on board Salyut-6 under the Intercosmos Programme /Vorobyov and Kovalyov, 1983/. Some of the Salyut-7 data was taken using the Hungarian "Pille" TLD system and has a considerably higher accuracy /Akatov et al., 1984/. In Fig. 2 is shown the range of average dose-rates (mrad-day) measured on board Salyut-7 in various positions within the spacecraft during the three measuring sessions of 36, 28 and 49 days duration. The numbers shown in Fig. 2 represent the lowest and the highest average dose-rate measured during these three sessions in each position. The measurements, which were performed in the second half of 1983, show that for Salyut-7 as well as for Salyut-6 spacecraft, in this particular orbit, the largest ratio of dose-rates within the spacecraft was about 1.6.

The highest dose-rates were found in the passage section on the left (16-23 mrad/day), and in one of the sleeping areas on the right (17-21 mrad/day). This was only a few feet away from the position of the work station on the right which recorded the lowest dose-rate of 13-15 mrad/day.

2.2 Joint U.S./Soviet Measurements

In addition to the manned space program, the Soviets have utilized the Cosmos Biosatellite series in order to conduct radiation experiments. As of this writing, eight such missions have flown, including Cosmos Nos. 110, 605, 782, 936, 1129, 1154, 1667, and 1887.

Four sets of radiation measurements using passive detectors were carried out jointly on the Cosmos Biosatellite series including Cosmos 782, 936, 1129 and 1887. The results for two of the flights are shown in Table 4 /Benton et al., 1983/. Here are shown the TLD dose and mission dose rate as well as neutron measurements made using a set of fission foils (described later). The results from Cosmos 1887 mission are in the initial stages of readout and analysis. Since the highest inclination orbit flown to date by the Space Shuttle is 57°, these joint Cosmos Biosatellite missions represent the highest inclination orbits available to the U.S. experimenters, and hence are useful in measuring the contribution to the total radiation picture of the galactic cosmic ray (GCR) component.

2.3 Measurements Under Thin Shielding

The objectives of the Cosmos missions are many and also include the development of new types of active shielding as well as dose measurements under very low shielding conditions. Fig. 3 shows a "waffle-iron" type of container which is mounted on the outside of the spacecraft and which holds various types of detectors. Once in orbit, the container is opened to the

734

Table 2. Absorbed and Equivalent Radiation Doses for the Crews of Salyut 3-6 Spacecraft*

Orbital Station	Trans-portation Spacecraft	Period and duration of flight	Astronaut	Radiation Dose	
				Absorbed $(10^{-5}$ Gy)	Equivalent (rem)
Salyut-3	Soyuz-14	3-19 July 1974, 16 days	P. Popovich Yu. Artyukhin	265±10 295±17	0.40 0.44
Salyut-4	Soyuz-17	11 Jan-9 Feb 1975, 30 days	A. Gubarev G. Grechko	770±110 640±80	1.1 1.0
	Soyuz-18	24 May-26 Jul 1975, 63 days	P. Klimuk V. Sevastyanov	3050±300 2170±190	4.6 3.3
Salyut-5	Soyuz-21	6 Jul-24 Aug 1976, 49 days	G. Volynov V. Zholobov	830±70 820±30	1.2 1.2
	Soyuz-24	7-25 February 1977, 18 days	V. Gorbatko Yu. Gladkov	348±12 338±9	0.52 0.51
Salyut-6: Expedition I	Soyuz-26	10 Dec 1977-16 Mar 1978, 96 days	Yu. Romanenko G. Grechko	2050±100 2150±80	3.1 3.2
II	Soyuz-29 and Soyuz-31	16 Jun-2 Nov 1978, 140 days	V. Kovalyonok A. Ivanchenkov	3150±190 3350±200	4.7 5.0
III	Soyuz-32 and Soyuz-34	25 Feb-19 Aug 1979, 175 days	V. Lyakhov V. Ryumin	3670±190 3670±190	5.5 5.5
IV	Soyuz-35 and Soyuz-37	9 Apr-11 Nov 1980, 185 days	L. Popov V. Ryumin	2700±160 2700±160	4.0 4.0
V	Soyuz-T4	12 Mar-26 May 1981, 75 days	V. Kovalyonok V. Savinykh	1100±40 1060±40	1.6 1.6

*/Vorobyov and Kovalyov, 1983./

Table 3. Individual Radiation Doses Incurred by Members of International Crews on board Salyut-6 Spacecraft under the Intercosmos Programme*

Astronaut	Country	Trans-portation Spacecraft	Date of Launch	Radiation Dose	
				Absorbed $(10^{-5}$ Gy)	Equivalent (rem)
A. Gubarev V. Remek	USSR Czechoslovakia	Soyuz-28	2 March 1978	250±23 260±9	0.38 0.39
P. Klimuk M. Germaszewski	USSR Poland	Soyuz-30	27 June 1978	188±18 201±16	0.28 0.30
V. Bykovsky S. Ien	USSR GDR	Soyuz-31 and Soyuz-29	26 August 1978	238±32 270±13	0.36 0.40
V. Kubasov B. Farkas	USSR Hungary	Soyuz-36 and Soyuz-35	26 May 1980	---- 135±20	---- 0.20
V. Gorbatko Fam Tuan	USSR Vietnam	Soyuz-37 and Soyuz-36	27 July 1980	190±25 216±22	0.28 0.32
Yu. Romanenko A. Mendez	USSR Cuba	Soyuz-38	18 Sept. 1980	150±15 147±15	0.22 0.22
V. Janibekov Zh. Gurragcha	USSR Mongolia	Soyuz-39	22 March 1981	165±15 182±16	0.25 0.27
L. Popov D. Prunariu	USSR Romania	Soyuz-40	14 May 1981	166±23 200±22	0.25 0.30

*/Vorobyov and Kovalyov, 1983./

| Cosmos Flight No.	936	1129
Flight duration (days)	18.5	18.56
Inclination	62.8	62.8
Altitude (km, apogee/perigee)	419/224	394/226
TLD dose (mrad)	474	347 (US) 320 (USSR)
TLD dose rate (mrad/day)	25.6	18.0
Thermal Neutrons		
fluence	3.6×10^5 cm^{-2}	5.1×10^5 cm^{-2}
dose	0.37 mrem ± 20%	0.52 mrem ± 20%
Resonance neutrons		
fluence	1.2×10^6 cm^{-2}	1.4×10^6 cm^{-2}
dose	6 mrem − 30% + 50%	7.4 mrem − 30% + 50%
High energy neutrons		
fluence	2.1×10^6 cm^{-2}	2.1×10^6 cm^{-2}
dose	125 mrem ± ?	125 mrem ± ?

/Benton et al., 1983/
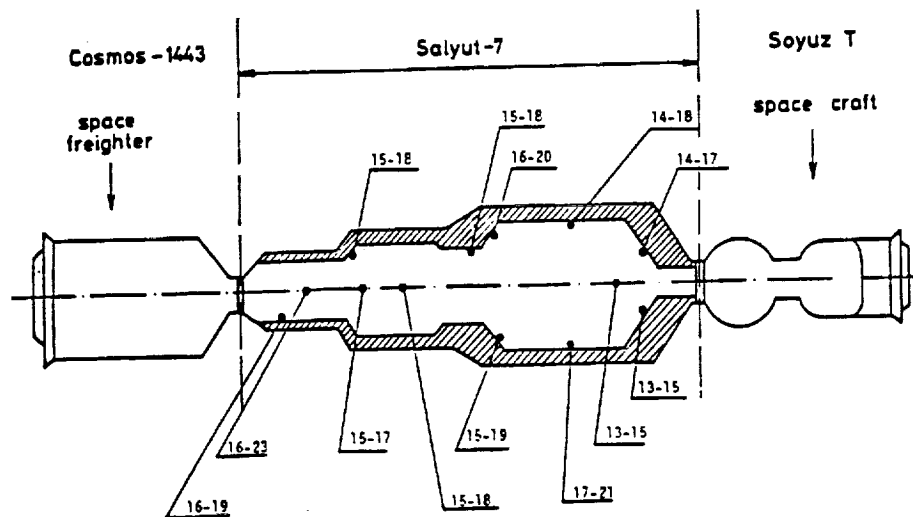
Fig. 2. Range of average dose rates (mrad/day) on board Salyut-7.
/Akatov et al., 1984./

free space environment. Absorbed dose as a function of thin shielding for Cosmos 936 and 1129 is shown in Fig. 4 /Benton et al., 1981/. Here, absorbed dose decreases three to four orders of magnitude in the first $\sim$(1-3) g/cm^2 of material /Dudkin, 1987; Benton, 1987/. Since this means that very thinly shielded portions of the spacecraft can receive very large radiation exposures, these measurements need to be verified for the various orbits and

Fig. 3. "Waffle-iron" detector container used on
Soviet Cosmos Biosatellite flights.

conditions so as to get a better picture of this environment. The rapid change in dose at these shielding depths is primarily due to absorption of low energy electrons.

2.4.1 Early measurements. The U.S. spacecraft used in manned space exploration are shown in Fig. 5 and include the Mercury, Gemini, Apollo, Skylab, the ASTP and the Space Shuttle, all shown roughly to scale. TLD mission dose and dose-rate data measured on the early U.S. manned space missions are shown in Table 5. The data for the Gemini, Skylab and ASTP flights reflect strongly the altitude dependence of these low Earth-orbital (LEO) missions, while the Apollo series reflects the specific path through the radiation belts on the way to and from the moon. Until fairly recently, the dose-rate of some 86 +/- 9 mrad/day for the Skylab-4 mission represented the
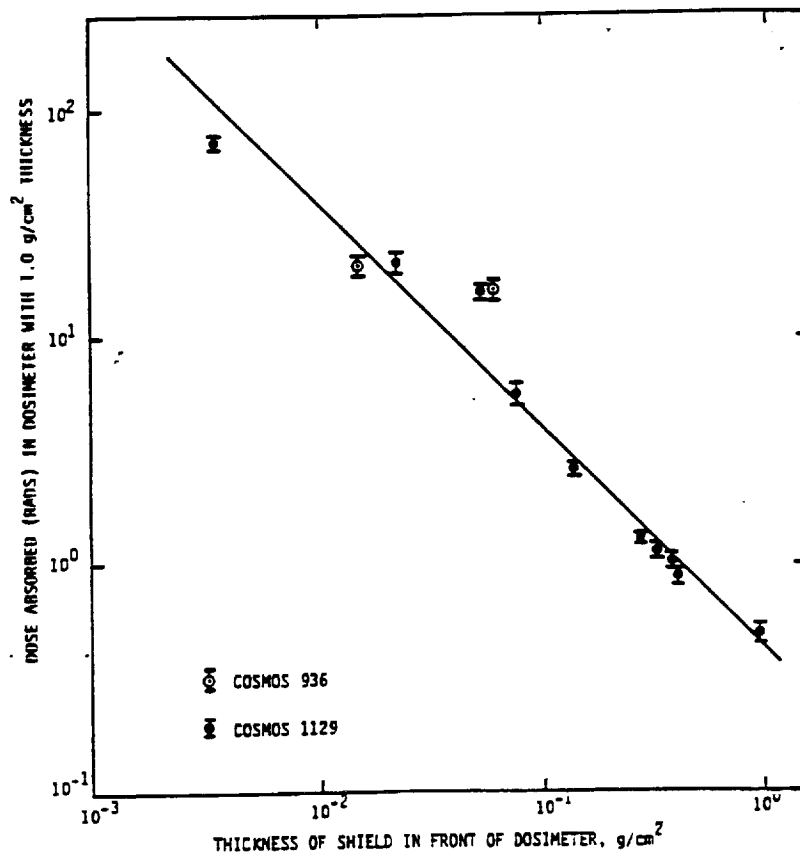

Fig. 4. Dose absorbed by dosimeter 1.0 g/cm² thick, as a function of shield thickness.
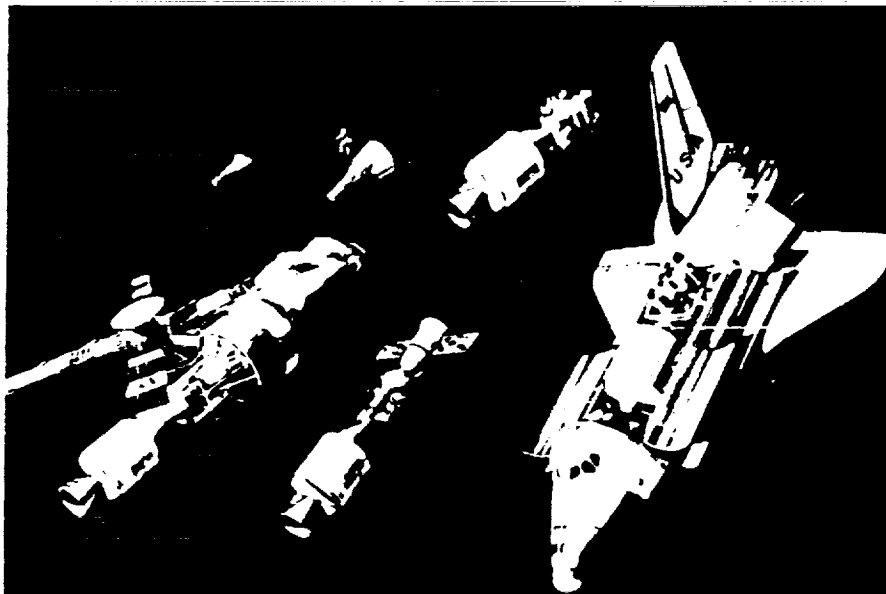
Fig. 5. Six types of U.S. manned spacecraft shown nearly to scale. (Clockwise from top left) Mercury, Gemini, Apollo, Space Shuttle, Apollo-Soyuz, Skylab.

Table 5. Crew Dose Rates from Early Manned U.S. Spaceflights

Flight	Duration (hrs/days)	Inclination (deg)	Apogee-Perigee (km)	Average Dose (mrad)	Average dose rate (mrad/day)
Gemini 4	97.3 hrs	32.5	296 - 166	46	11
Gemini 6	25.3 "	28.9	311 - 283	25	23
Apollo 7*	260.1 "			160	15
Apollo 8	147.0 "		lunar orbital flight	160	26
Apollo 9	241.0 "			200	20
Apollo 10	192.0 "		lunar orbital flight	480	60
Apollo 11	194.0 "		lunar flight	180	22
Apollo 12	244.5 "		" "	580	57
Apollo 13	142.9 "		" "	240	40
Apollo 14	216.0 "		" "	1140	127
Apollo 15	295.0 "		" "	300	24
Apollo 16	265.8 "		" "	510	46
Apollo 17	301.8 "		" "	550	44
Skylab 2**	28 days	50	alt = 435	1596	57 ± 3
Skylab 3	59 days	50	alt = 435	3835	65 ± 5
Skylab 4	90 days	50	alt = 435	7740	86 ± 9
Apollo-Soyuz Test Project	9 days	50	alt = 220	106	12

*Doses for the Apollo flights are skin TLD doses. The doses to the blood-forming organs are approximately 40% lower than the values measured at the body surface.
**Mean TLD dose-rates from crew dosimeters.
†Apollo data courtesy of J. V. Bailey /1977/.

highest dose-rate recorded by any astronaut while in low Earth-orbit /Bailey 1977/. The average crew dose-rates recorded on Apollo lunar missions ranged from 22-127 mrad/day and that recorded on Apollo 14 (127 mrad/day) is still the highest mission-average crew dose-rate recorded to date. The average dose-rates inside the heavily shielded film vault drawers B (16-30 g/cm^2) and F (30-50 g/cm^2) of Skylabs 2 and 3 were 39.5 and 33.4 mrad/day[1] respectively.

2.4.2 <u>STS measurements</u>. The passive dosimeters which were used on the Space Shuttle missions STS 1-61C, which include the crew passive dosimeter or CPD (which consists of the TLD module and the module containing a set of PNTDs), as well as three pencil-type, electrometer-type dosimeters, having ranges of 0-200 mrad, 0-100 rad, and 0-600 rad, are shown in Fig. 6. The plastic box at the bottom left is that of the area passive dosimeter (APD) which was flown on the first several missions and which contained, in addition to the TLDs and PNTDs, some fission-foil-type, low-energy neutron dosimeters. The APD and the electrometers are fitted into the pouch shown at the bottom right of the picture.

The TLD crew passive dosimeter data from the first twenty-four flights of the Shuttle are shown in Table 6. The doses and mission dose-rates reflect for the most part the low-LET components of the radiation. It is observed that the first eight flights of the Shuttle, which involved orbiters Columbia and Challenger and which had similar orbits of 28.5° to 40° inclination and nominal altitudes of 250-300 km, all showed very modest mission dose-rates of 5-7 mrad/day. With the first flight of the Spacelab, Spacelab-1 (STS-41A), in an orbit having about the same altitude but an inclination of 57°, the dose-rate doubled to about 12 mrad/day. From these measurements and those of Parnell et al., /1986/, we now know that, at most locations in the Shuttle or Spacelab, the bulk of the dose recorded on this type of low-altitude, 57° inclination flight is the result of GCR.

Parnell et al., /1986/, showed that on Spacelab-1, at a shielding depth of ∿ 8 gm/cm^2, only about 15% of the dose was attributable to the trapped protons of the South Atlantic Anomaly (SAA). This situation changed dramatically with the flight STS-41C, the Solar Max repair mission which, although at orbital inclination of 28.5°, was the first true higher altitude mission, with a maximum of ∿528 km and recording a mission-average crew dose-rate which was an order of magnitude greater than the nominal low-altitude flights, namely, about 74 mrad/day. In this case it is clear that the bulk of the dose comes from the SAA, with the GCR contributing something of the order of 5-6 mrad/day. Starting with flight STS-41G and continuing until the most recent flight, STS-61C, the missions showed dose-rates of 11-22
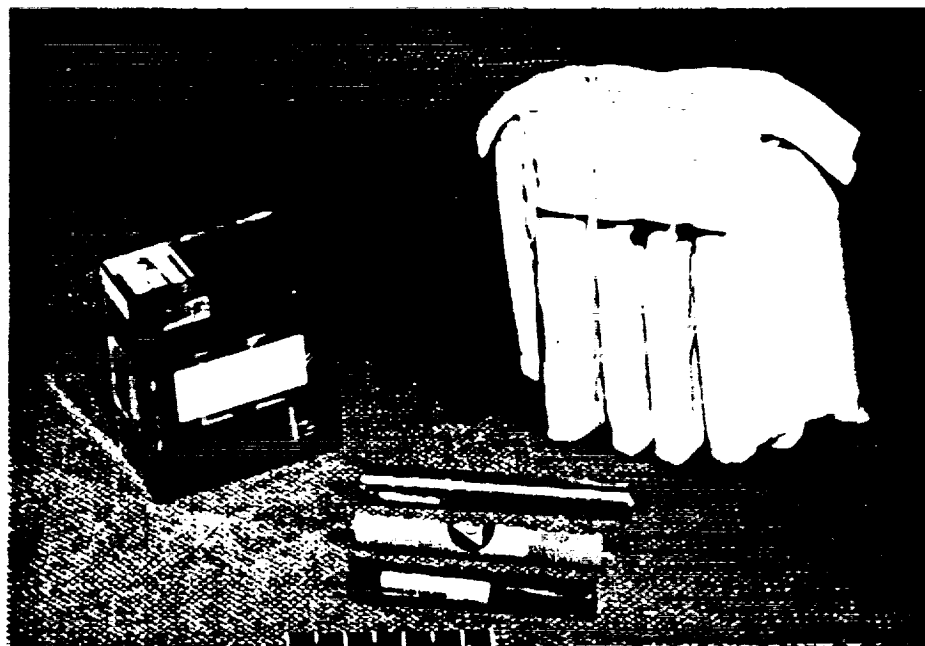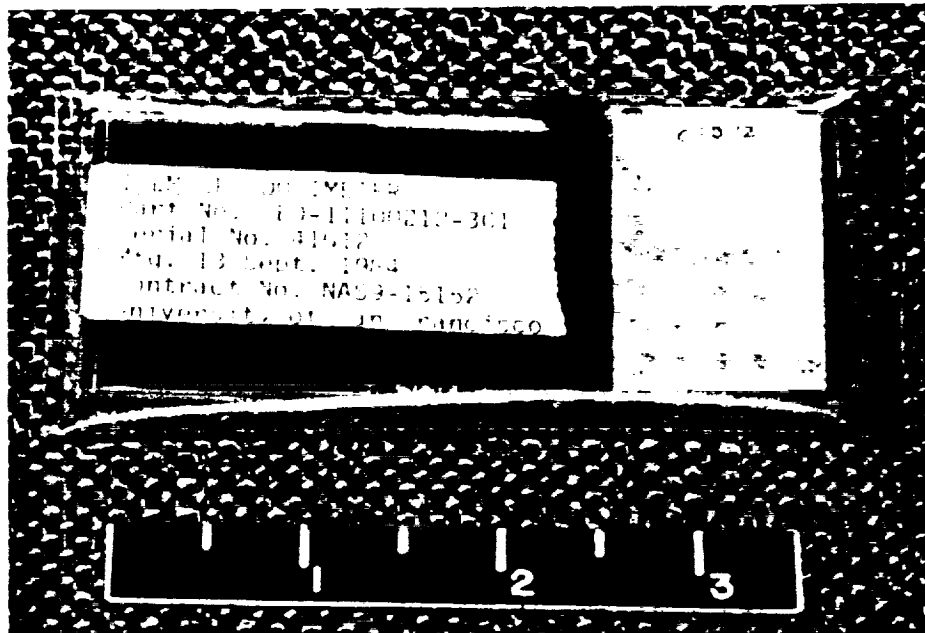
Fig. 6.

Top: STS Crew Passive Dosimeter

Bottom: Area Passive Dosimeter and three electro-
meter-type dosimeters with the pouch which
holds the instruments.

Table 6. Crew Doses and Mission Parameters for the Space Shuttle Flights[*]

STS Mission Number	Spacecraft	Launch Date	Mission Duration (hr)	Alt. (km)	Inc. (°)	Number of Crew	Range of Crew Doses (mrad)	Average Crew Dose (mrad)	Ave. Crew Dose Rate (mrad/day)
1	Columbia	04-12-81	54	269	40	2	not avail.	8.9	4.0
2	Columbia	11-12-81	58	254	38	2	6-11(USF)	8.5±2.3(USF)	3.6
3	Columbia	03-22-82	195	280	38	2	50-52(USF)	50.9±0.7(USF)	6.3
4	Columbia	06-27-82	169	297	28.5	2	44-45(USF)	44.4±0.2(USF)	6.3
5	Columbia	11-11-82	122	284	28.5	4	27-29(USF)	27.8±1.2(USF)	5.6
6	Challenger	04-04-83	120	293	28.5	4	24-27	25±2	5.0
7	Challenger	06-18-83	143	297	28.5	5	43-46	44±1	7.4
8	Challenger	08-30-83	145	297(max)	28.5	5	38-41	39±1	6.5
41A	Columbia	11-28-83	248	250	57	6	119-141	125±2	12.1
41B	Challenger	02-03-84	191	297	28.5	5	45-49	48±1	6.0
41C	Challenger	04-06-84	168	528(max)	28.5	5	443-622	519±5	74.1
41D	Discovery	08-30-84	145	297	20.5	6	51-53	52±1	8.6
41G	Challenger	10-05-84	197	352(max)	57	7	84-92	88±1	10.7
51A	Discovery	11-08-84	192	297x352	28.5	5	80-159	115±2	14.4
51C	Discovery	01-24-85	74	297x334	28.5	5	35-41	39±1	12.6
51D	Discovery	04-12-85	168	297x454	28.5	7	303-472	381±5	54.4
51B	Challenger	04-29-85	166	352	57	7	127-160	148±2	21.4
51G	Discovery	06-17-85	170	380(max)	28.5	7	105-152	130±1	18.4
51F	Challenger	07-29-85	191	322x304	49.5	7	112-167	138±2	17.3
51I	Discovery	08-27-85	192	378(max)	28.5	5	99-120	106±1	13.3
51J	Atlantis	10-03-85	95	510(max)	28.5	5	329-513	426	107.8
61A	Columbia	10-30-85	169	324	57	8	112-139	121	17.2
61B	Atlantis	11-26-85	165	380	28.5	7	125-171	143	20.8
61C	Columbia	01-12-86	146	324	28.5	7	65-75	69	11.3

[*] Stated uncertainty represents measurement precision, 1σ of the mean, rather than absolute accuracy. Previous measurements of absolute accuracy suggest that the given values are accurate to within 6-8%. Data for missions STS-1 through STS-5 supplied by the University of San Francisco; remainder supplied by the Radiation Dosimetry Laboratory, NASA-Lyndon B. Johnson Space Center.

mrad/day; however, most of these flights involved changes in altitude. By looking at the average crew dose-rate after a mission, it is possible to ascertain whether a higher-than-300 km altitude orbit was involved. For example, mission 51J, the first flight of Atlantis, with orbital inclination of 28.5° and a maximum altitude of 510 km, recorded an average crew dose-rate of 107.8 mrad/day, which is now the highest average crew dose-rate recorded by any crew while in low Earth-orbit. There is a steep dose-rate gradient, increasing with altitude above ∿300 km. The dose does not change as dramatically with inclination between 28.5° and 57°, where the variation is about a factor of 2. At the lowest altitudes (∿250 km) the dose increases with inclination due to the increased cosmic ray flux at higher geomagnetic latitudes. At the higher altitudes (400-500 km) the dose would be maximum near 35° inclination, since the spacecraft spends more time in the peak region of the SAA. It should also be noted that in higher-inclination orbits the LET spectrum is shifted towards the higher values.

The steep dose gradient with altitude and the changing energy spectrum of trapped protons which are responsible for most of the dose (at altitudes ∿500 km) was clearly observed in the data of Atwell et al., /1987a/. The devices used were flown beginning with mission STS-6 and continuing through STS-61C with six Passive Radiation Detectors (PRDs) deployed at specific locations in the spacecraft. Each PRD, which weighs about 25 grams and contains 32 TLD chips, is attached to the same specific location each time by means of a Velcro strip. PRD Nos. 1, 2 and 3 are located on the inside of the outer periphery of the mid-deck, while PRD Nos. 4, 5 and 6 are located on the inside of the outer periphery of the flight deck (see Fig. 7). The shielding at these six locations differs significantly (see Fig. 8) /Atwell and Beever, 1987b/. Location No. 1 is the most heavily shielded of the six, while location No. 2 is the least shielded. The data for STS missions 6-24 are shown in Figs. 9 /Benton, 1986/ and 10 /Atwell et al., 1987a/. For missions 6 through 41B the dose-rate for the six locations is very similar, as seen from the clustering of the data from the six detector locations (see Fig. 9). The dose-rate points spread out considerably for the three high-altitude missions, 41C, 51D and 51J. Here, in each case, location No. 2, which is on the mid-deck on the left wall facing aft, consistently gives a substantially higher dose-rate than position No. 1 which is also on the mid-deck, just above the payload bay air-lock. The ratio of dose-rates between position No. 2, as compared to location No. 1, was as high as 2.2. In location No. 2 was recorded the highest mission dose rate measured inside the orbiter, ∿200 mrads/day, on STS-51J. The PRD data for only the 28.5° incli-
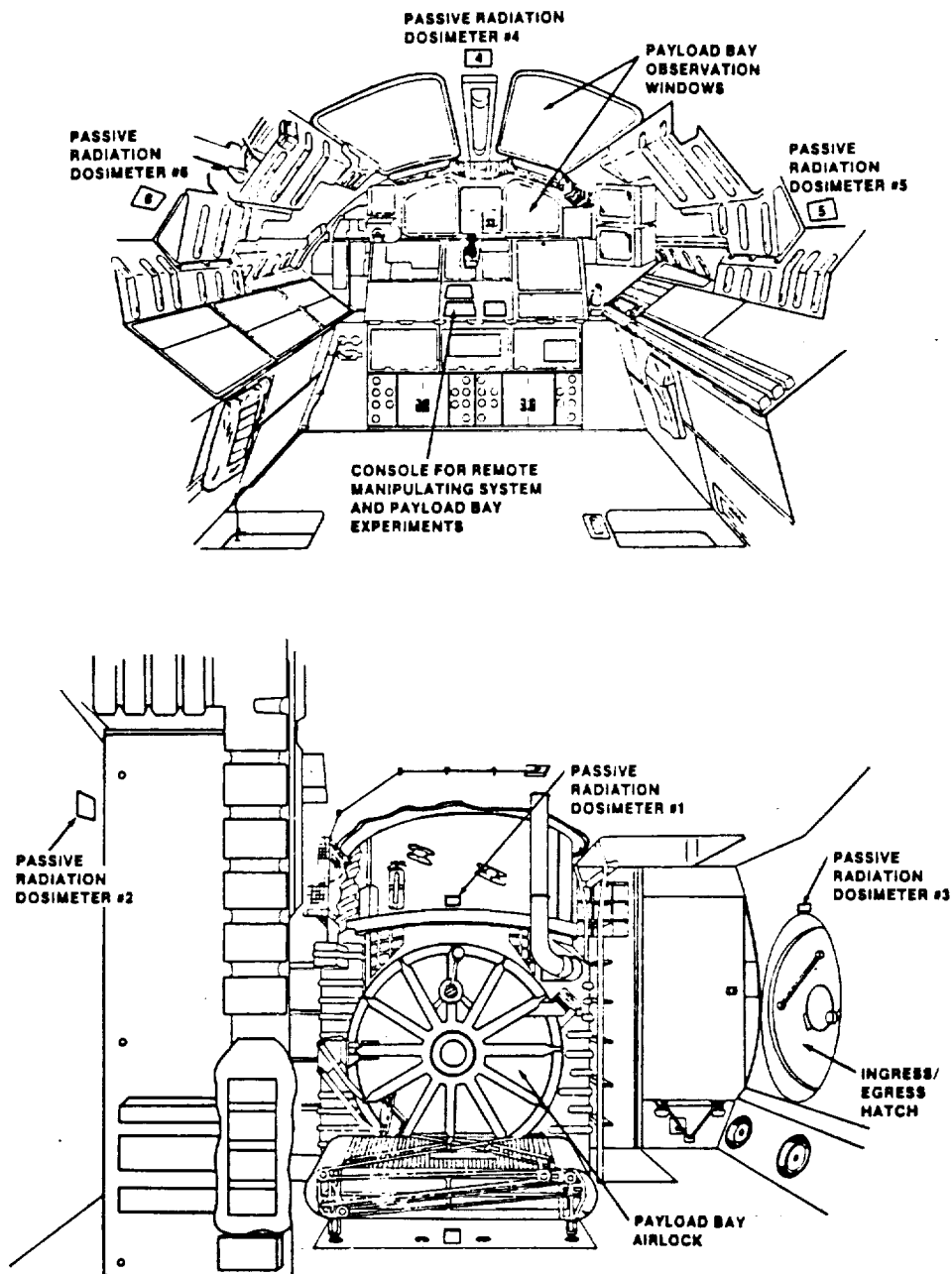
743

PASSIVE RADIATION
DOSIMETER #4
[4]

PAYLOAD BAY
OBSERVATION
WINDOWS

PASSIVE
RADIATION
DOSIMETER #6

PASSIVE
RADIATION
DOSIMETER #5
[5]

[6]

CONSOLE FOR REMOTE
MANIPULATING SYSTEM
AND PAYLOAD BAY
EXPERIMENTS

PASSIVE
RADIATION
DOSIMETER #1

PASSIVE
RADIATION
DOSIMETER #2

PASSIVE
RADIATION
DOSIMETER #3

INGRESS/
EGRESS
HATCH

PAYLOAD BAY
AIRLOCK

Fig. 7. Passive Radiation Detector locations on Space Shuttle.
Top: aft flight deck
Bottom: aft mid-deck
/Atwell et al., 1987a/

744

nation flights was plotted as a function of orbital altitude and compared with calculations for solar minimum and solar maximum (see Fig. 10) /Atwell et al., 1987a/.

Measurements performed with the APDs on STS-1 through 51C and giving the mission dose-equivalent are shown in Table 7. Here, the TLDs used were of the 700 type. The high LET portion of the LET spectrum was measured using the six orthogonally-positioned stacks of CR-39 detectors. This was needed in order to take account of the strong directionality of the plastic detectors. The neutron measurements were made using ^{6}LiF and ^{232}Th foils positioned against CR-39 and mica detectors, respectively (as discussed later).
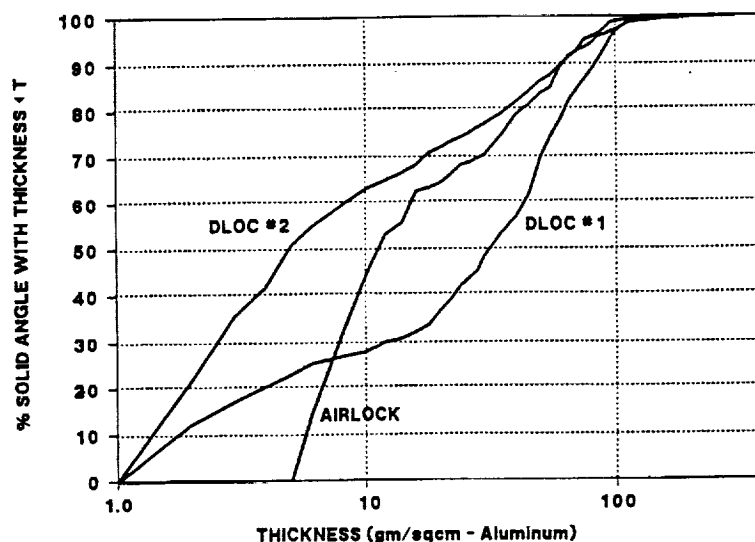
Fig. 8. STS orbiter shield distributions for PRD locations No. 1, 2, and the airlock /Atwell and Beever, 1987b/.

The dose-equivalent for the high LET ($\gtrsim$ 20 keV/μm H_2O) particles as measured by the CR-39 detectors was obtained by integration of the integral LET spectra with the use of the appropriate quality factors as recommended by the ICRU (see Note 1). The low LET dose is obtained by taking the TLD data and subtracting from it the high LET absorbed dose as measured by plastic detectors. Then the.total mission rem dose is obtained through the addition of the low LET, the high LET, and the neutron contributions (see Table 7). Because of some unusual behavior of the plastic track detectors experienced during the early flights (prior to STS-41B), the reported high LET rem doses may be somewhat (10-20%) higher than actual. LET measurements are discussed more completely in Section 5.0.
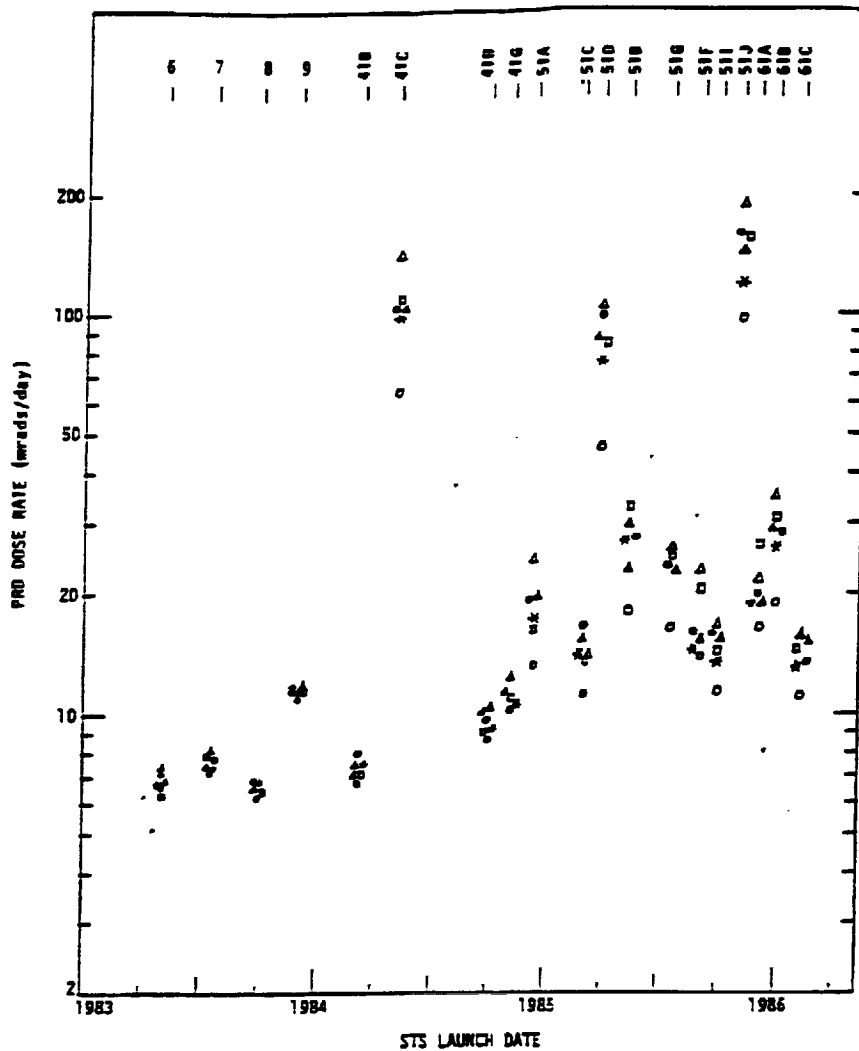
Fig. 9. The dose rate in mrad/day obtained by flying the six PRDs on
missions STS-6 through 61C, as a function of launch date.
Data courtesy of R. Richmond, NASA-JSC.

Key: PRD-1 (○ — on airlock, above hatch)
PRD-2 (△ — on outer wall behind and aft DFI)
PRD-3 (□ — on outer wall, above ingress/egress hatch)
PRD-4 (* — aft, toward CL of observation window)
PRD-5 (● — on closeout panel above locker L-10)
PRD-6 (▲ — on closeout panel above locker R-11)

Table 7. Space Shuttle Dosimetry Summary: Measurements from the Area Passive Dosimeters

	Whole-Body Dose Equivalents (mrem)			
	STS-1	STS-2	STS-3	STS-4
LOW-LET*		12.5 ± 1.8	52.5 ± 1.8	44.6 ± 1.1
Rate (/day)		5.2 ± 0.8	6.5 ± 0.2	6.3 ± 0.2
Neutron				
Thermal	< 0.05	< 0.03	0.03	0.04
Resonance	< 0.75	< 0.3	2.0	1.6
High Energy	----	----	7.7	14
Total	< 15	< 6	9.7	15.6
HIGH-LET**	3.6 ± 0.4	1.0 ± 0.4	6.3 ± 1.0	7.7 ± 2.9
Total Mission				
Dose Equivalent		< 19	68.5	67.9
Mission Parameters				
Storage Locker				
Duration (hrs)	54	57.5	194.5	169.1
Inclination (deg)	38	38	40.3	28.5
Altitude (km)	240	240	280	297

	STS-5	STS-6	STS-7	STS-8
LOW-LET*	27.8 ± 2.5	27.3 ± 0.9	34.3 ± 2.3	34.8 ± 1.3
Rate (/day)	5.6 ± 0.5	5.5 ± 0.2	5.8 ± 0.4	5.8 ± 0.2
Neutron				
Thermal	0.03	0.03	0.02	0.02
Resonance	0.7	1.9	1.4	2.6
High Energy	11	6.5	----	----
Total	11.7	8.4	1.4***	2.6***
HIGH-LET**	14.5 ± 1.6	13.8 ± 1.8	11.7 ± 1.6	19.2 ± 3.5
Total Mission				
Dose Equivalent	54.0	49.5	47.9***	56.6 ± 3.7***
Mission Parameters				
Storage Locker	MF140	MF28K	MF28K	MA16F
Duration (hrs)	120	120	143	70 75
Inclination (deg)	28.5	28.5	28.5	28.5
Altitude (km)	297	284	297	297 222

	STS-9	STS-41B	STS-41C	STS-41D
LOW-LET*	101.1 ± 3.1	43.6 ± 1.8	403 ± 12	42.0 ± 2.8
Rate (/day)	10.1 ± 0.3	5.5 ± 0.2	57.6 ± 1.7	7.0 ± 0.5
Neutron				
Thermal	0.1	0.02	0.05	0.01
Resonance	2.2	0.5	3.1	1.5
Total***	2.3	0.5	3.2	1.5
HIGH-LET**	76.3 ± 9.2	13.6 ± 1.5	98 ± 3	21.3 ± 1.3
Total Mission				
Dose Equivalent***	179.7 ± 9.7	57.7 ± 2.3	504 ± 12	64.8 ± 3.1
Mission Parameters				
Storage Locker	MF28E	MF280	MF280	MF280
Duration (hrs)	240	191	168	145
Inclination (deg)	57	28.5	28.5	28.5
Altitude (km)	241	297	519	297

	STS-41G	STS-51A	STS-51C
LOW-LET*	82.4 ± 2.4	94.3 ± 4.9	35.4 ± 2.0
Rate (/day)	10.0 ± 0.3	11.3 ± 0.6	11.5 ± 0.6
Neutron			
Thermal	0.03	0.04	---
Resonance	1.1	0.9	---
Total***	1.1	0.9	---
HIGH-LET**	71.0 ± 2.8	37.3 ± 2.3	12.2 ± 2.1
Total Mission			
Dose Equivalent**	154.5 ± 3.7	133.0 ± 5.3	47.6 ± 2.9
Mission Parameters			
Storage Locker	MF280	MF280	MF280
Duration (hrs)	29/19/148.5	192	73.6
Inclination (deg)	57.0	28.5	28.5
Altitude (km)	352/274/224	324	297-334

*Photons and electrons of any energies. High LET at lower efficiency.
**HZE particles with LET >20 keV/um of water.
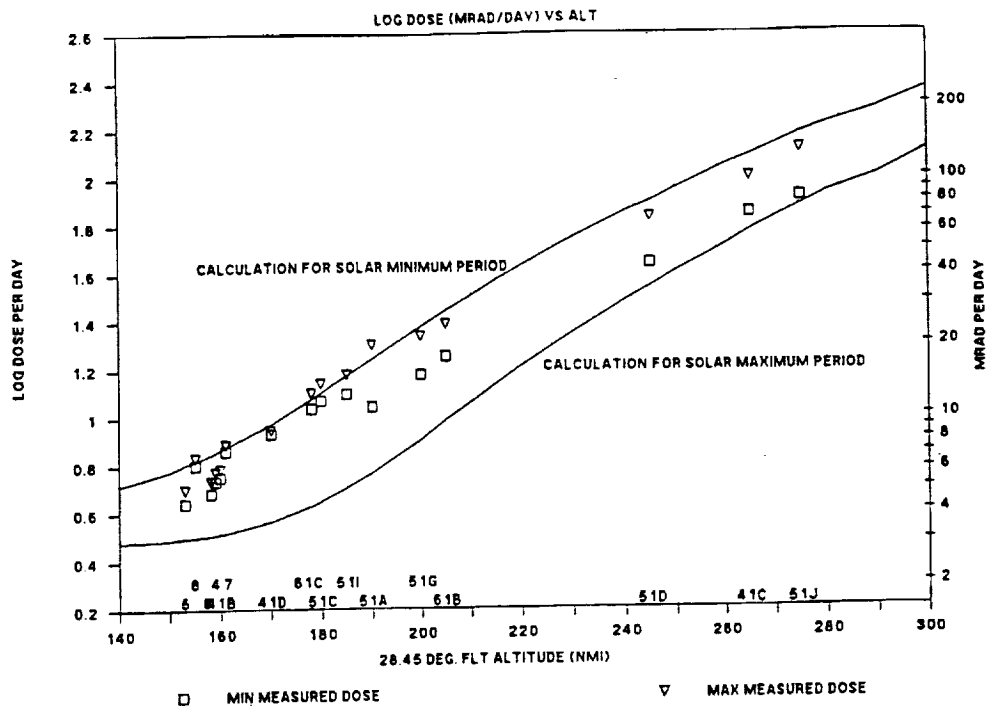*** Does not include high-energy neutron dose.

LOG DOSE (MRAD/DAY) VS ALT

CALCULATION FOR SOLAR MINIMUM PERIOD

CALCULATION FOR SOLAR MAXIMUM PERIOD

28.45 DEG. FLT ALTITUDE (NMI)

□   MIN MEASURED DOSE   ▽   MAX MEASURED DOSE

Fig. 10.   STS PRD dose measurements/calculations /Atwell et al., 1987a/.

3.0 ACTIVE DETECTORS FOR DOSIMETRY

Active, real time detectors play an important role in radiation measurements in that they allow the determination of temporal changes in the radiation environment, provide information on dose and flux rates, and can allow the separation of dose contributions from the different components, i.e., GCR, trapped protons, electrons and bremsstrahlung, etc. Relatively few active dosimetry-related measurements to date have been made in the U.S. manned space program.

The Soviets have flown a number of active instruments in their manned program, but very little information is available in the literature concerning either instrumentation or results. They have, however, reported LET spectra from Cosmos 782, 986, and 1129, from a particle spectrometer. These results are discussed in Section 5.0.

3.1 Early Measurements on Gemini and Apollo

Beginning with the Gemini program, a variety of ion chamber dosimeters and solid state detector "dosimeters" were developed and carried on the Gemini and Apollo flights. The chambers were generally of the tissue-equivalent

748

ion chamber (TEIC) type, the principles and construction of which are des-
cribed by Janni /1976/. These detectors and some of the measurements have
been summarized /Janni, 1969b; Schneider and Janni, 1969; Richmond, 1969/.
The data was often subject to telemetry and other limitations, so synoptic
data on missions are not always available. Nevertheless, some pioneering
results are still very useful for comparison with more recent data. Their
usefulness is an indication of the paucity of recent measurements and also
the utility of TEIC measurements. For Gemini IV (163 x 281 km, 32.5^0), mea-
surements were published for orbits outside the SAA, and peak dose rates in
the SAA /Schneider, 1969/. Two TEICs were carried, mounted inside each
hatch, which had minimum shielding of >1 g/cm^2 of aluminum over large solid
angles. One TEIC was demountable and was used to survey the effects of
equipment and self-shielding around the crew members' bodies /Schneider and
Janni, 1969/. At the highest geomagnetic latitudes, dose rates up to 0.18
μrads/s due to GCR were recorded. In the center of the SAA, dose rates up
to 35 μrads/s were obtained, an indication of the thin shielding and the in-
fluence of the artificial electrons from the Starfish explosion three years
before.

The two TEICs on Gemini IV also indicated the directionality of the SAA
trapped particles by indicating doses that varied in opposite directions by
a factor of >2 while the spacecraft changed attitude. Table 8 lists major
features of the Gemini IV data compared with that from similar TEICs carried
on Skylab and Spacelab-1, to be discussed in the next two sections.

Gemini VI (259, 328 x 161 km, 29^0) used the same ion chambers, one with
a 2.5 g/cm^2 brass shield. This one-day mission varied in altitude, with the
apogee out of the SAA. The shielded chamber showed doses lower by a factor
of two, compared to the unshielded chamber in the SAA, with interesting
variations due to the directionality of the trapped flux.

The Apollo program carried a complement of dosimeters similar to Gem-
ini /Richmond, 1969/. Because of the short time the lunar missions spent
in the trapped belts, the majority of these doses were from cosmic rays (see
Section 2.4). However some of the Apollo flights passed near the maximum
trapped proton flux region. Apollo VI TEICs recorded maximum doses of 10^3
μrads/s (3.6 rad/hr) and 720 μrads/s (2.6 rad/hr) for the "skin dose" and
"depth dose," with two ion chambers in the command module.

3.2 Skylab Results

Skylab (415 km, 50^0) carried a rather comprehensive set of passive de-
tectors available at the time and also active instruments /Janni, 1976/.
The passive detectors were TLDs (CaF$_2$, LiF), nuclear track emulsions, plas-

Table 8. Dose Measurement from Gemini IV, Skylab and Spacelab-1
Measured with Tissue-Equivalent Ion Chambers (TEICs)

	Dose-rates in microrads/second		
	Max. CR[†]	Av. CR	Max. SAA
Gemini IV (281x161 km, 32.5°)	0.18	0.047	35*
Spacelab-1 (250 km, 57°)	0.28	0.110	1.7
Skylab II (415 km, 50°)	0.55	0.055	23

*Note shielding of Gemini IV TEIC ($\gtrsim$ 1 gm/cm²), flown three years after Starfish
†Cosmic rays

tic nuclear track detectors, activation foils, and quartz fiber electro-scopes. The active detectors were TEICs and a small two-detector solid state particle telescope to measure LET spectra. The instrumentation is completely described in Janni /1976/. The TEIC chamber was designed accor-ding to the Bragg-Gray principles (to provide accurate results in a mixed radiation field) and constructed of approximately tissue-equivalent plastic and filling gas. Results from the Skylab-2 mission TLD measurements and some TEIC results are contained in Janni /1976/, including numerous passes through the South Atlantic Anomaly. Dose rates up to 23 μrads/s were re-corded in the center of the SAA. Outside the anomaly, dose rates averaged about 0.055 μrads/s due to cosmic rays, which increased to ∿0.55 μrads/s at the highest geomagnetic latitudes. At the geomagnetic equator the dose rate was as low as ∿0.014 μrads/s. These values may be compared with the average mission·dose measured by the TLDs of about 0.5 μrads/s (1.2 rads for the 28-day mission).

3.3 Coordinated Active and Passive Measurements, Results from SL-1 and SL-2

An example of the usefulness of even very simple active devices when coordinated with passive detector arrays is the work by Parnell et al. on SL-1 and -2 /1986/. Two Active Radiation Detector (ARD) packages were flown on SL-1, each containing an integrating TEIC (see Refs., Note No. 2) and two xenon-filled proportional counters (see Refs., Note No. 3, and Figs. 11 and 12). These simple omnidirectional detectors were flown to measure tem-poral variations of radiation dose and count-rate due to cosmic ray nuclei, trapped protons and electrons, and bremsstrahlung X-rays from electrons. The ion chambers had a sensitive gas volume of 180 cm³. Preflight calibra-
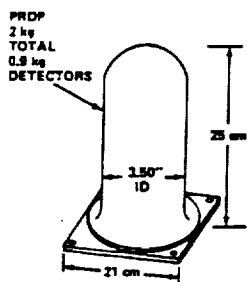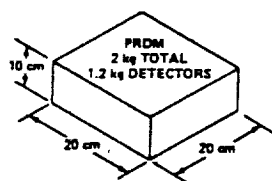
tions of the ion chambers were reproduced after the flight within 5 percent. The proportional counters (PCs) had a sensitive volume of $\sim$60 cm^3 and counted each ionizing event with energy deposition greater than 5.9 keV in the gas (about 85% of the charged particles and 2% of 100-keV photons). In the laboratory the PC count rate was $\sim$1/s. One PC in each unit was surrounded by a copper sleeve 1 g/cm^2 thick which would absorb 40% of 100-keV photons. The ARDs were placed in the top and bottom of equipment rack No. 3 in the SL-1 module. Passive detector packages containing TLDs, PNTDs, neutron fission foils, activation samples, and nuclear track emulsions were placed beside each active detector and at other locations in the Spacelab module.

The Spacelab-1 mission flew for 10 days at $\sim$250 km altitude and 57^0 inclination. Twenty-nine passive and two active detector packages were used at a variety of shielding locations in the module and tunnel, and one passive unit was on the pallet.

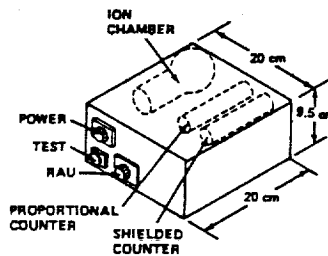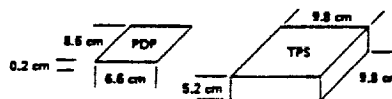## SPACELAB 1 RADIATION MEASUREMENT PACKAGES

Fig. 11. Detector package configurations for Experiment INS006 and Verification Flight Instrumentation (VFI) on Spacelab-1 /Parnell et al., 1986/.

The average ion chamber dose rates were 12.5 ± 0.7 and 12.8 ± 0.7 mrads/day in the top and bottom of rack No. 3. TLD measurements in adjacent PRD-Ms registered 9.7 ± 0.3 mrad/day and 10.9 ± 0.3 mrad/day, respectively. The ior chambers thus appear to measure about 20% higher values than the TLDs. Part of this is due to the TLDs' lower sensitivity to heavy nuclei. As determined from the ion chambers and proportional counters, about 85% of the SL-1 module dose comes from cosmic rays, and the TLDs are less sensitive to very heavy nuclei than singly charged particles. Other contributions to the difference may be systematic biases in calibration and biased environment sampling due to data gaps, which existed for about 45% of the mission.
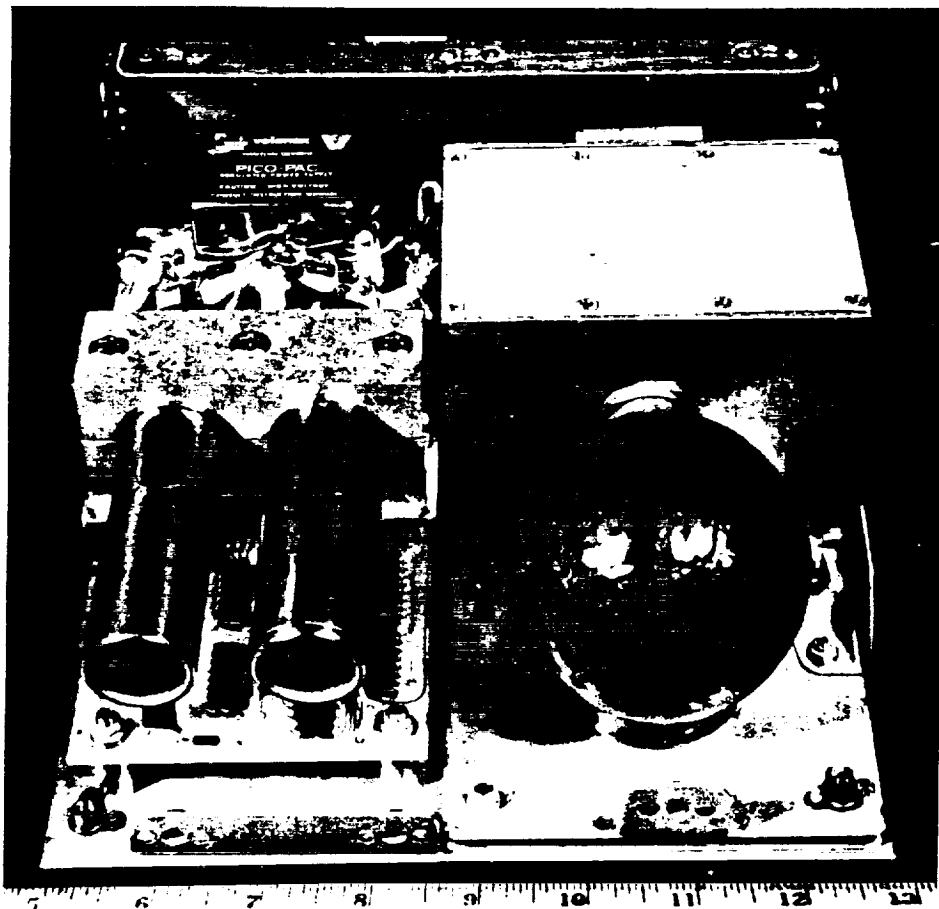

Fig. 12. Active Radiation Detector (ARD) package flown on Spacelab-1, containing an integrating tissue-equivalent ion chamber and two xenon-filled proportional counters.

752

The temporal information from the ion chambers and proportional counters allowed an assessment of the relative contributions of the cosmic rays and trapped belt particles. Fig. 13 is a one-hour segment of data from one ion chamber and the two PCs in the same unit. This shows variations in the integrated ion chamber dose and PC rates due to cosmic rays (with the expected geomagnetic dependence as the spacecraft travelled from north to south); this effect and the trapped particles in the SAA region and the south "horn" of the electron belt are shown in Fig. 14. The small "bump" of electrons in the middle are probably transiently trapped on those field lines. The observation that the ion chamber dose rates in the south horn region are not significantly different from rates at other high latitude portions of the orbit (see Fig. 15) shows that the high PC rates there are due to bremsstrahlung photons produced by electrons stopping in the Spacelab structure. In Fig. 15, one can see the effect of the copper shield on one PC in absorbing ∿40% of the photons. The high PC rates in the SAA are mostly due to the trapped protons that produce the increase in ion chamber (IC) dose rate in that region. The similar proportional counter rates in the SAA and electron horn regions are an artifact of the orbit and the sensitivity of the xenon-filled PC to photons.

The segments of the ion chamber data indicating the SAA (see Figs. 14 and 15) by temporal behavior of the PC count rate comprise 0.13 of the average mission dose for the top ion chamber and 0.10 for the one in the bottom of rack No. 3. These fractions may be somewhat biased by data gaps, but show clearly that the dose in the SL-1 orbit is dominated by the cosmic rays, as predicted by pre-flight calculations /Watts and Wright, 1976/. Those calculations also predict that trapped protons would dominate above ∿350-400 km for similar locations in the Spacelab module.

Occasionally at large geomagnetic latitudes, sudden increases in proportional counter rates occurred as shown in Fig. 16. Bremsstrahlung photons of ∿100 keV characteristic energy are indicated by the relative count rates of the shielded and unshielded PCs and the lack of significant ion chamber dose rate above that expected from cosmic rays. The intensity was occasionally approximately twice that observed in the undisturbed south electron horn and episodes lasted from a few to ∿500 s. Seventeen significant episodes occurred in five days of ARD data. These events resemble trapped electron "precipitation" events previously observed /Imhof et al., 1979 and 1986/. These bremsstrahlung photons are generated by electrons stopping in the atmosphere and are probably seen from large distances.

The low fraction of dose due to trapped particles in the SL-1 module makes assessment of the trapped environment and its absorption by shielding
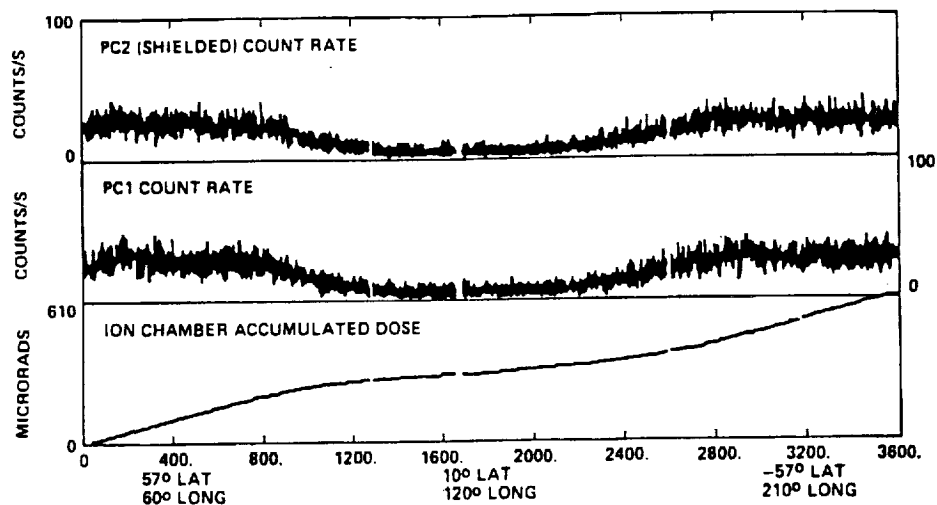
Fig. 13. One-hour segment of data from one ion chamber and two proportional counters in the same unit. Variations in ion chamber dose integration and PC rates due to cosmic rays are shown.
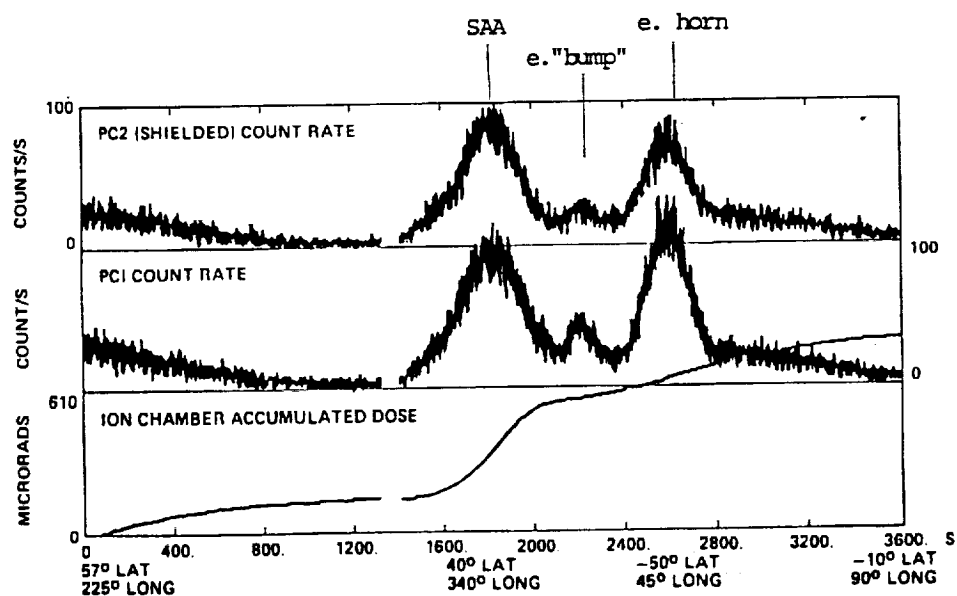

Fig. 14. Effect of geomagnetic dependence as spacecraft travels north to south and of trapped particles in the SAA region, the electron "bump", and the south horn of the electron belt. Note effect of shielding between the two counters.

somewhat uncertain. Analysis is also complicated by the short mission and variation in attitude of the Shuttle because the trapped particle angular distribution is directional, with more particles arriving nearly perpendicular to magnetic field lines in a "pancake" distribution /Heckman and Nakano, 1963; Watts et al., 1987/. To aid in assessing the SAA and south electron horn effects, contour maps of the radiation were assembled. The maps were constructed by averaging data around geographical points (e.g., within $3°$), and smoothing. Displayed in Fig. 17 are the rates from two ICs and one of
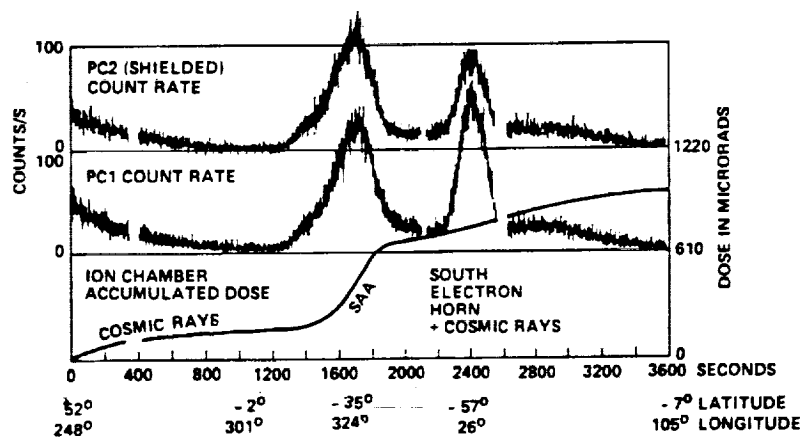

Fig. 15. Count rate of two proportional counters and ion chamber accumulation at high northern latitudes, the geomagnetic equator, the SAA, and the electron horn.
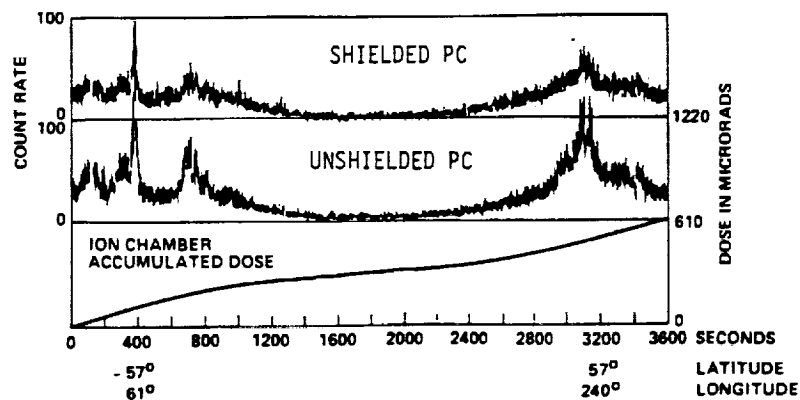

Fig. 16. One hour of ARD data in which the SAA and electron horns are not encountered. Large fluctuations in the PC count rates are likely due to electron precipitation.

the PCs in the SAA region. That the two ICs are in different shielding situ ations is obvious. Comparisons between the maps show high PC count-rates in the south electron horn region, but the ICs have no significant dose accumu- lation there. This is due to the relatively high sensitivity of the xenon- filled PCs to bremsstrahlung photons as previously noted. The averaging pro· cess reduced the maximum dose and count-rate contours displayed ~20% below the actual values.

The 29 passive packages all contained TLDs and plastic track detectors and were designed to map the low and high LET dose in the Spacelab module. Some passive packages carried fission foil detectors for neutrons, metal samples for activation analysis and nuclear track emulsions to record the entire LET spectrum. This array of passive packages at 29 locations would have been prohibitive to implement with active detectors and it provided spe- cific information on radiation components of interest in a number of contexts including the determination of the biological dose-equivalent (neutrons, HZE particles), and activation of sample materials.

The large number of passive detectors at different locations, the mea- surement of the different environment constituents, and the temporal infor- mation from the active detectors presented an extensive survey of the radi- ation environment within SL-1. Cosmic rays produced most of the dose at all locations in the Spacelab module. Only at a few detector locations was the dose significantly above that expected from the cosmic rays alone. This was due to the large shielding depths ($\sim$14-66 g/cm^2 arithmetic average) of the Spacelab-Orbiter structure, and the low altitude. Detectors that had low shielding depths (< 1.5 g/cm^2) over significant solid angles ($\sim$8% of 4 pi sr) registered the largest doses in the module. For these detectors, the frac- tion of the measured dose attributable to trapped particles was about one- half the calculated values. This might indicate that the environmental model flux is too high. However, the trapped flux is directional, which is not in the model, and caution must be observed in such comparisons.

The steep trapped electron and proton spectra cause small solid angles about detectors subtended by light shielding (< 2 g/cm^2) to dominate the trapped particle dose component. Thus a "dose-weighted shield," calculated with the available trapped environment models, was found convenient to place the measured doses in order with respect to shielding. For a massive space- craft such as this, an accurate vector shield model is necessary before accurate doses can be predicted. The directional characteristics of the ambient radiation may also need to be used. These considerations become par- ticularly important at altitudes above 350-400 km where the trapped compo- nent is dominant and the proton energy spectrum is softer.

756

17(a) — IC-1

17(b) — IC-2

17(c) — PC-11
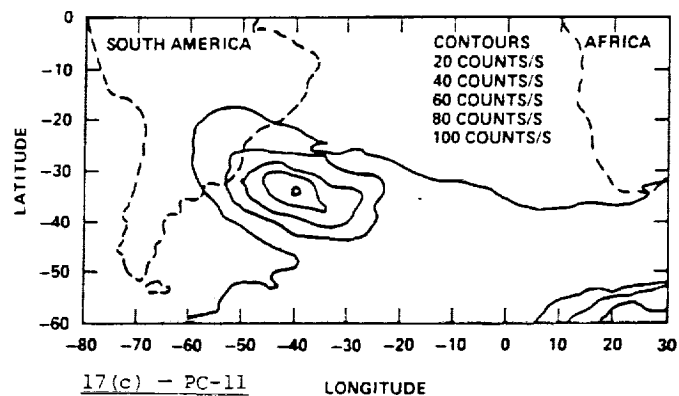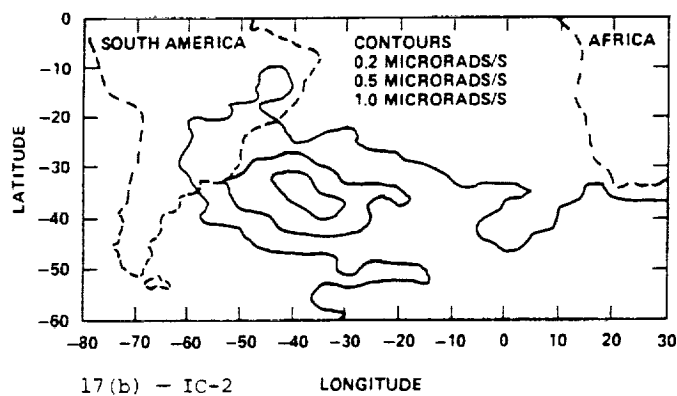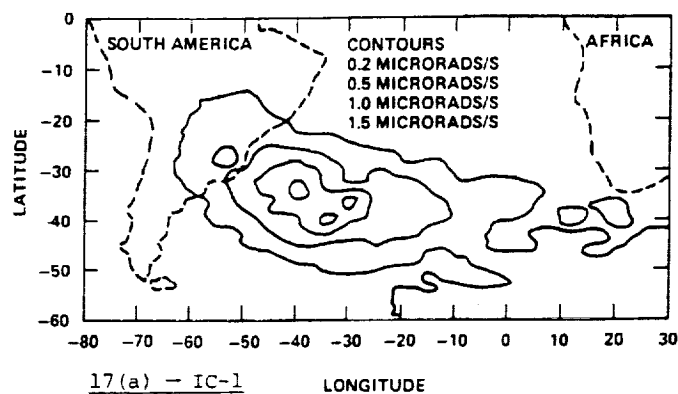
Fig. 17. Maps of dose isocontours in the SAA for ion chambers
1 and 2. The PC count rate for the counter in ARD 1
(unshielded) is also shown. Dose rates for the ion
chamber in the top of rack 3, shown in 17(a), are higher
in the center of the SAA than for the one in the bottom
of rack 3, shown in 17(b). The contours of the propor-
tional counter 17(c) show high rates in the south horn,
near longitude 30°E /Parnell et al., 1986/.

3.4 Active Dosimetry Instruments on Unmanned Spacecraft

Since Explorer I discovered the Van Allen Belts, a large number of spacecraft have carried instruments of varied sophistication to directly measure the flux, spectra, spatial distribution and temporal variations of the trapped particles. Some products of these extensive data were the models of the spatial distribution, energy spectra, and major temporal features of the trapped protons and electrons. The most widely used models are those maintained by the National Space Science Data Center (NSSDC) at NASA/GSFC. The current models, AP8MIN, AP8MAX /Sawyer and Vette, 1976/, and AE8MIN, AE8MAX /Vette and Chen, 1987/, have superseded earlier versions /Vette, 1966; Singley and Vette, 1972; Teague and Vette, 1974; Chan et al., 1976, 1977/. The trapped radiation environment is discussed in Stassinopoulos /1987/.

Some unmanned missions have carried instrumentation specifically designed for measurements of dosimetric quantities. Generally these unmanned spacecraft and the instruments have considerably less shielding than the manned missions, but in most cases the shielding is more accurately known. The unmanned spacecraft have covered high altitude and polar orbits where data is not available from manned missions (except Apollo transits).

The OV spacecraft series was contemporary with Gemini and early Apollo flights. A variety of electronic radiation instruments were flown on some OV spacecraft including particle telescopes, single silicon detectors in spherical shielding, and TEICs on some flights. Considerable data from these missions are described in an issue of Aerospace Medicine /Janni, 1969c; Thede 1969/. These missions performed significant surveys of the environment and dose rates at altitudes between ~425 and 5000 km and in polar orbits. They investigated the temporal variations of the outer belt electrons and disturbances due to solar flares.

The OV1-2 (413 x 3078 km, 144°) carried three silicon solid state dosimeters and two TEICs under light shielding (up to 5 gm/cm^2) and an X-ray detector. Iso-dose and count-rate data were presented /Radke, 1969/ over the complete B-L space covered by the orbit.

OV1-4 (886 x 1012 km, 144.5°) carried three lightly shielded (1.3-2.6 gm/cm^2) TEICs. Iso-dose contours in B-L coordinates and geographic maps were presented. Dose rates of 80 rads/hr (2.2 x 10^4 μrads/s) from the TEICs were seen at the center of the SAA at 956 km. The inner radiation belt was still enhanced by electrons from the Starfish explosion, which had occurred about four years before the data was taken. In these data the anisotropy of the trapped radiation was noted in changes of dose-rate as the spacecraft rotated.

The OV1-12 mission (309x428 km, 102°) carried three TEICs with shielding of 0.3, 0.8 and 2.7 g/cm^2. They gave peak rates of 2.7x10^3, 1.39x10^3 and 0.83x10^3 μrads/s in the SAA and 1.6-9.7x10^3, 0.07x10^3, and a "trace" of μrads/s in the cusps of the outer belt. These data clearly showed the large temporal variability of the electron flux in the outer belt.

OV19 (470x5,677 km, 104.7°) carried a variety of active detectors including LET spectrometers and three TEICs under 0.3, 5.0 and 12.0 g/cm^2 shields /Cervini, 1971/. Data was reported from orbits during "quiet" times and following solar flares. The thinly shielded chamber gave rates from 2.8 x10^2 μrads/s at low altitudes to saturation of 1.7x10^5 μrads/s below the maximum altitude. Following solar flares at the higher altitudes, the most heavily shielded chamber gave rates up to 3.3x10^3 μrads/s.

Much of the OV radiation data was compared to environment models by Thede /1969/ and Vette /1966/. Although there was influence from the Starfish electrons in the inner belt, these comparisons did provide valuable information on the status of the proton models.

More recently, the Defense Meteorological Satellite Program (DMSP-F7) has carried silicon detector "dosimeters" on a nearly polar orbit at 840 km /Mullen et al., 1987/. The four small silicon detectors are covered with hemispherical aluminum shields of 0.55, 1.55, 3.05, and 5.91 g/cm^2. The energy deposition thresholds on the detectors are set so that rather good separation between electrons and protons is achieved. The data is also binned so that energy depositions due to heavy cosmic ray nuclei, and evaporation or recoil nuclei from nuclear interactions in the the detector, fall in a bin called VH LET or "star events." These events are of interest in predicting soft faults" in microcircuits and are caused by densely ionizing particles that would have a high relative biological efficiency (RBE).

The analyzed proton and electron spectral data (from 1984) was compared to calculations using the latest electron and proton models from the NSSDC. The proton data agreed with the calculations rather well and the electron results were a factor of ∿2 low compared to the models. The DMSP data displayed the temporal fluctuations of the outer zone electrons and the geographic distribution of the SAA protons and outer zone electron "cusps" at 840 km. A global "star" count map clearly showed the importance of the SAA protons in producing high LET events through recoil or interaction, and showed the geographic distribution of such events due to cosmic rays.

The above short description of some results from active dosimeters on unmanned spacecraft indicates the value of such data which covers much of the high altitude, high inclination regime not yet available from manned missions.

4.0 HZE PARTICLE INTEGRAL FLUX -- APOLLO AND SKYLAB

Over the past two decades, the research group at the University of San Francisco has been involved with measurement of high-LET particle radiation inside manned spacecraft. This work began with the observation of tracks of a few heavily ionizing particles in plastic nuclear track detectors flown aboard Gemini IV and Gemini VI in 1966 /Benton and Collver, 1967/. It became apparent from this work that a stack of a few layers of plastic films is a simple and direct means of measuring the integrated flux of heavy particles inside spacecraft. Plastic films are well-suited for such measurements; they are lightweight, rugged, and capable of recording and storing particle tracks over long periods of time with no loss of sensitivity and little latent track fading. Their inability to record lightly ionizing particles (i.e., electrons and protons with LET <6 keV/μm H_2O) permits registration of the relatively small number of heavy cosmic-ray nuclei in a high particle-radiation background situation such as exists in space.

By the start of the Apollo program, the field of dielectric nuclear particle track detectors was sufficiently developed that the first serious effort in the measurement of high-LET cosmic-ray particles could be carried out on Apollo missions. This was done on Apollo missions 8-17. Plastic nuclear track detectors recorded heavy particle radiation incident on astronauts /Benton et al., 1975a/ and several biological experiments /Benton et al., 1974/. The particle registration threshold for cellulose nitrate and Lexan detectors is approximately 80 and 225 keV/μm H_2O.

A detailed summary of results is presented in Table 9 /Benton et al., 1975a/. Dosimeters located on the astronaut's ankle consistently recorded a particle flux higher than those recorded by chest and thigh dosimeters. This is explained as due to less shielding of particles by the astronaut's body at the ankle region compared with the thigh and chest regions. An increase in particle flux was observed which correlates approximately with solar activity. The anti-correlation of the galactic cosmic ray flux below ∿5 GeV with solar activity is a well-recorded phenomenon, and the mechanism of solar modulation is still an active field of study /Marenny, 1987/. The high-LET particle flux in the last column shows that the flux on the Apollo 17 mission was ∿2.4 times that on the Apollo 8 mission.

Of this series, Apollo 17 was the most heavily monitored mission. In addition to personnel passive dosimeters, four biologically related experiments were instrumented to contain plastic nuclear track detectors. The four experiments included the HZE Dosimeter /Henke and Benton, 1974/, the Biostack /Bücker, 1975/, the ALFMED /Osborne and Pinsky, 1975/, and the Biocore /Haymaker et al., 1975/. Table 10 /Benton et al., 1975b/ summarizes

Table 9. Apollo Mission: HZE Particle Planar Fluences Derived from a Least Squares Analysis

(Particles /cm² with LET_{350} > 150 keV/μm in Lexan)*

Apollo mission No.	Command module pilot (only in spacecraft)			Commander and lunar module pilot (also on lunar surface)				Geometric mean fluence	Geometric mean flux (cm⁻²day⁻¹)
	Chest	Thigh	Ankle	Chest	Thigh	Ankle	Film bag		
8	2.3 ± 0.4	2.6 ± 0.4	3.2 ± 0.5				8.2 ± 0.9	3.2 ± 0.5	0.58 ± 0.09
10	2.8 ± 0.3	3.2 ± 0.4	3.9 ± 0.4				6.5 ± 0.7	4.0 ± 0.3	0.61 ± 0.05
11	2.4 ± 0.3	2.8 ± 0.4	3.4 ± 0.4	3.5 ± 0.3	3.2 ± 0.3	3.9 ± 0.4	5.5 ± 0.6	3.4 ± 0.3	0.50 ± 0.04
12	3.3 ± 0.4	3.7 ± 0.4	4.5 ± 0.5	4.7 ± 0.4	5.2 ± 0.4	5.2 ± 0.4	7.4 ± 0.8	4.6 ± 0.4	0.56 ± 0.05
13	3.1 ± 0.4	3.5 ± 0.5	4.3 ± 0.5	4.4 ± 0.5	4.0 ± 0.5	4.9 ± 0.5	7.1 ± 0.9	4.3 ± 0.5	0.74 ± 0.09
14	4.4 ± 0.5	5.1 ± 0.6	6.1 ± 0.6	6.3 ± 0.5	5.8 ± 0.5	7.1 ± 0.6	10.1 ± 1.0	6.2 ± 0.5	0.83 ± 0.07
15	6.9 ± 0.7	7.9 ± 0.8	9.6 ± 1.0	9.9 ± 0.7	9.0 ± 0.6	11.1 ± 0.8	15.8 ± 1.3	9.7 ± 0.6	1.07 ± 0.07
16	8.2 ± 0.9	9.3 ± 1.1	11.3 ± 1.2	11.7 ± 0.9	10.7 ± 0.9	13.1 ± 1.0	18.7 ± 1.8	11.5 ± 0.9	1.38 ± 0.11
17	9.4 ± 0.8	10.7 ± 1.0	13.0 ± 1.0	13.4 ± 0.7	12.2 ± 0.7	15.0 ± 0.7	21.4 ± 1.3	13.2 ± 0.5	1.41 ± 0.05
Position factor	0.71 ± 0.05	0.81 ± 0.06	0.98 ± 0.06	1.02 ± 0.05	0.93 ± 0.05	1.14 ± 0.05	1.63 ± 0.05	—	

*LET_{350} includes only energy transfer with secondary electron energy <350 eV (equivalent to LET_∞ tissue >225 keV/μm).

761

Table 10. Apollo 17: HZE Particle Track Fluences[a]

| Experiment | Detector layer number | Measured | | Absolute planar track fluence (tr cm^{-2}) | | Flux[d] (tr cm^{-2} day^{-1}) |
		2 cones	Etched-through holes	LET$_{350}^{CN}$ >170 keV μm^{-1} [b]	LET$_{350}^{CN}$ >80.0 keV μm^{-1} [c]	LET$_{80}^{CN}$ >80 keV μm^{-1}
HZE dosimeter (2 g cm^{-2})	C5	108.5	30.8	26.1 ± 3.9	153 ± 23	16.4
Biostack (10 g cm^{-2})	E2-1	60.7	19.4	16.2 ± 2.3	95 ± 14	10.2
	E13-25	55.0	18.0	13.4 ± 1.8	78 ± 11	8.4
Alfmed (~ 20 g cm^{-2})	bottom sheet	26.6	14.7	11.7 ± 1.5	69 ± 9	7.4
Biocore[e] (30–40 g cm^{-2})	implanted mouse brain dosimeters	31.0	8.7	7.0 ± 1.6	41 ± 9	4.4

[a] All measurements are from cellulose nitrate of the type USF 4b processed for 10.0 hr at 40 C in 6.25 N NaOH.
[b] Corresponds to an LET$_{350}^{Lexan}$ > 150 keV μm^{-1} in Lexan or LET$_x^{tissue}$ ≥ 225 keV μm^{-1}.
[c] Corresponds to an LET$_{80}^{tissue}$ ≥ 105 keV μm^{-1}.
[d] Flux is in effective days in interplanetary space; mission duration 301.5 hr or 9.33 effective days.
The Biocore numbers are average for the four live mice.

the data from these experiments. The influence of shielding is observed, with the lightly shielded HZE dosimeter recording nearly four times the flux recorded by Biocore detectors. Even for the heavily shielded Biocore, there is a significant flux of high-LET particles. This underscores the point that complete shielding from the galactic cosmic rays is not practical due to spacecraft weight limitations.

The radiation environment of the Skylab missions differed significantly from that of the Apollo lunar missions. Being a near-Earth orbital mission, the Skylab was shielded both by the physical presence of the Earth and by the geomagnetic field. Measurements of high-LET particles incident on Skylab personnel, film vault /Benton et al., 1977/ and command module /Peterson and Benton, 1975/ were made using thin plastic films which for the first time included a more sensitive detector (LET $\simeq$ 80 keV/μm H_2O), cellulose nitrate, as well as Lexan. In the command module, five plastic nuclear track dosimeters were distributed around the interior. The results of these measurements are shown in Table 11 for the nine astronauts, the two drawers (B and F) in the film vault, and the five positions inside the command module.

Table 11. Skylab: HZE Particle Exposure

Mission (duration)	Astronaut	(1)	Observed $\left(\dfrac{particles}{cm^2}\right)$	Planar fluence $\left(\dfrac{particles}{cm^2\ 2\pi\ sr}\right)$ (2)	(3)	Planar flux $\left(\dfrac{particles}{cm^2\ day\ 2\pi\ sr}\right)$ (2)	(3)
SL2 (28 days)	C. Conrad	~5–10	55	54	15	1.9	0.5
	J. Kerwin		45	65	5.4	2.3	0.2
	P. Weitz		41	52	5.4	1.9	0.2
SL3 (59.5 days)	A. Bean	~5–10	126	181	7.10	3.04	0.12
	O. Garriott		143	145	18.1	2.44	0.30
	J. Lousma		136	165	20.3	2.77	0.34
SL4 (84 days)	J. Carr	~5–10	211	274	29.6	3.26	0.35
	E. Gibson		206	315	11.2	3.75	0.13
	W. Payne		183	255	26.0	3.04	0.31
Film vault	Drawers						
SL1-2[a]	B	~16–30	19	27	2.9	0.70	0.075
SL1-3[b]	B		32	79	11	0.59	0.079
SL1-2[a]	F	~30–50	13	14	1.4	0.36	0.036
SL1-3[b]	F		31	42	4.0	0.31	0.030
Command module	Detector						
SL2 (28 days)	1	~3–14	58.2	93.8	11.5	3.35	0.41
	2	~1–24	35.1	27.5	4.3	0.98	0.15
	3	~3–20	26.1	21.1	2.6	0.75	0.093
	4	~3–22	53.4	85.9	8.7	3.07	0.31
	5	~1–20	52.8	37.0	8.6	1.32	0.31

[1] Estimated shielding (g cm^{-2} Al).
[2] $LET_{350} \geq$ 80 keV μm^{-1} CN^{-1} (i.e. $LET_\infty \geq$ 105 keV μm^{-1} tissue^{-1}).
[3] $LET_{350} \geq$ 170 keV μm^{-1} CN^{-1} (i.e. $LET_\infty \geq$ 225 keV μm^{-1} tissue^{-1}).
[a] 39-day exposure.
[b] 134.5-day exposure.

The average planar flux incident on Skylab astronauts is 2.0, 2.8 and 3.4 particles cm^{-2} day^{-1}, respectively, for the SL2, SL3 and SL4 missions. The flux increase anti-correlates well with solar activity and may also be due in part to a decrease in spacecraft shielding as expendables such as water, food and propellant were used up. The heavily shielded film vault drawers received a much lower flux of high-LET particles. Detectors in film drawer F ($\sim$50g cm^{-2}) recorded flux up to an order of magnitude lower than that recorded for the astronauts.

5.0 LET SPECTRA

The LET spectral information is needed in determining the appropriate quality factors for the radiations present /Heinrich, 1977; Curtis and Benton, 1980/. To date, a few measurements of integral LET spectra have been made during actual space flights or in orbiting satellites. The earliest measurements of LET spectra were made by the Soviets on Soyuz and Salyut flights using nuclear emulsions /Benton et al., 1974; Benton, 1983/. More recent measurements of LET spectra on Cosmos 782, 936 and 1129 involving the use of electronic spectrometers, emulsions and plastic track detectors /Akopova et al., 1985/, are shown for comparison purposes in Fig. 18. Integral LET spectra as a function of LET_∞ in water is shown for the four Soviet experiments and several spectra measured by this laboratory on various U.S. manned space flights. Soviet spectra labeled Nos. 2 and 3 (Cosmos 782 and 936 respectively) were obtained using electronic spectrometers, spectra No.1 (Cosmos 1129) using special nuclear emulsions, while spectra No. 4 measurements were made on Cosmos 936 using PNTDs. The emulsions used were of a special type which have a controlled registration threshold in six discrete steps and operate in a range of 1-1000 keV/μm. The emulsions record protons up to $\sim$50 MeV. The most recent spectra are those of Cosmos 1129, with the average shielding reported to be $\sim$20 g/cm^2. The LET spectra measured on Cosmos 936 using electronic detectors (Curve 3) and plastic track detectors (Curve 4) are in reasonably good agreement with each other /Akopova et al., 1985/. Shielding of electronic detectors on Cosmos 782 (Curve 2) was only about 1 g/cm^2. This lower shielding on Cosmos 782 as opposed to Cosmos 1129 results in a substantial contribution to absorbed dose from the trapped protons of the SAA.

The more recent LET spectra measurements (Fig. 18) include those from three selected flights of the Space Shuttle including mission 51F (320-km flights of Spacelab-2 in a 49.5° inclination), a high-altitude mission of 51J (500 km at 28.5°) and the most recent flight of Columbia (STS-61C, 324 km, 28.5°). These three missions are fairly representative of the different
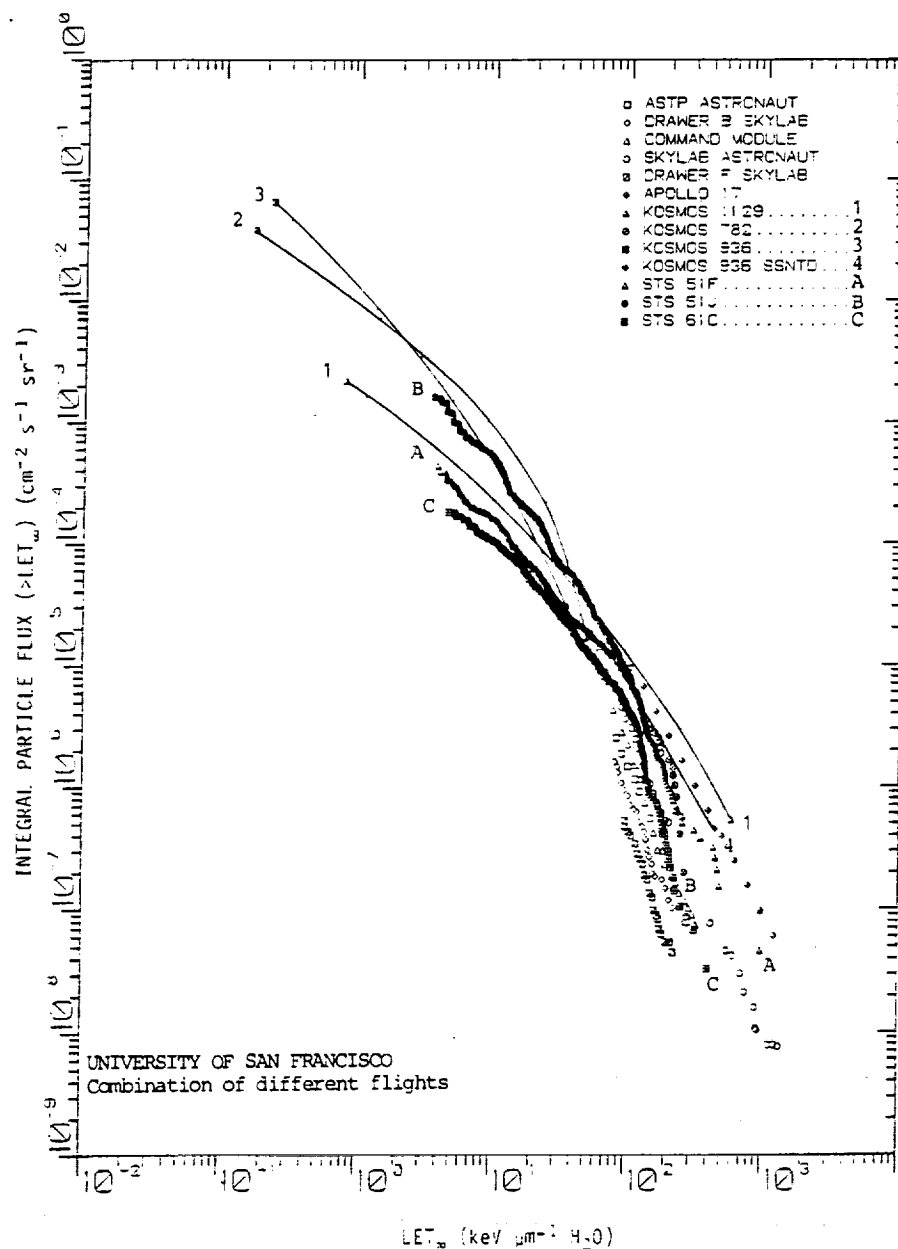
Fig. 18. Integral LET flux spectra showing number of particles as a function of LET∞ in water for various U.S. and Soviet flights.

STS mission types flown during the first 24 flights and the corresponding LET spectra are shown as curves labelled A, B and C in Fig. 18. All three spectra represent the average obtained from the five CPDs for each flight. Here, Curve A for STS-51F differs from a similar figure published previously /Benton, 1986b/ in that the previously-published spectra represented measurements obtained from a stack of detectors located on the pallet of STS-51F (Spacelab-2). The pallet location had considerably less shielding, resulting in a much flatter spectrum at the higher LETs ($\gtrsim$ 100 keV/μm). Presumably this is the result of lower energy (predominantly Fe nuclei) particles which get shielded out at the crew locations.

Curve C, mission STS-61C (324 km, 28.5°), represents the most typical low-altitude, low-inclination, 28.5° mission. This can be compared with Curve B, that of mission STS-51J, at the same inclination but a considerably higher altitude. Spectra B and C are similar in slope, with spectra B being considerably higher in the lower LET portion of the spectrum since most of the tracks here come from the trapped protons. On the other hand, Spectra A from STS-51F (Spacelab-2, ≤ 324 km, 49.5°) extends to greater LETs and is dominated by the contribution from GCR.

Measurements and/or calculations of LET spectra have also been performed by Heinrich /1977/, Letaw and Adams /1986/ and Adams et al. /1986/. Letaw /1986/ has calculated LET spectra for Skylab (Fig. 19). Here, CN and Lexan detector data include data from the crew, the command module, the two film drawers, and the calculations of Letaw and Adams /1986/. The calculated values were found to be consistently high by a factor of about two over the measured values. This disagreement also is present for their Apollo and the ASTP calculations. Work is now in progress aimed at reconciling measurements and calculations. In Fig. 20 is shown a comparison of LET spectra measured on STS-41G (352 km, 57°) by Adams /1986/ and Benton /1985a/, independently, using CR-39. Both sets of detectors were exposed in separate GAS canisters located in the cargo bay of the Shuttle under similar shielding conditions. Both sets of measurements as well as the calculations of Adams appear to be in a reasonably good agreement with each other, even though the calculations did not include heavy ion fragmentation. Since the amount of shielding was low ($\gtrsim$ 2.0 g/cm^2), the fragmentation effect could be neglected.

6.0 NEUTRONS INSIDE SPACECRAFT

Neutrons inside spacecraft are normally produced from interactions of GCR and trapped protons with the spacecraft material. Also there are some albedo neutrons from the atmosphere. The atmospheric albedo neutrons from cosmic ray interactions are the major source of inner belt protons and their

flux and spectrum have been calculated /Armstrong, 1973/ and also measured
at energies above 2 MeV /Bhatt, 1976; Lockwood, 1976/. Predictions dealing
with neutron levels inside spacecraft, taking the three sources into account
as well as the transport through the shielding, are not currently available.
However, a few measurements have been made (see Tables 12, 13 and 14)/Frank
and Benton, 1987/.

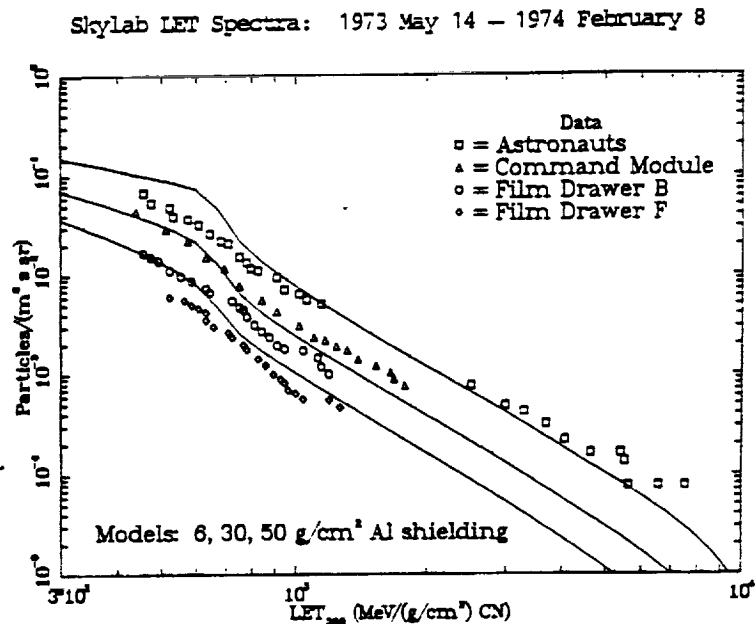Skylab LET Spectra: 1973 May 14 — 1974 February 8

Fig. 19. Calculated and measured LET spectra for the Skylab mission. Measurements from the astronauts' dosimeters and other positions within the spacecraft are shown. All calculations have been reduced by a factor of 2 to account for heavy shielding behind the detectors /Letaw and Adams, 1986/; Benton et al., 1977/.

The high neutron capture cross-section of ^6Li for thermal and resonant
neutrons provides a means of detection through the reaction of $^6Li(n,T)^4He$.
The alpha particle fluences emitted from the surfaces of ^6Li TLDs are recorded with the CR-39 plastic track recorder. The thermal neutron response is
separated from that of resonance neutrons by using Gd foil of 0.0025-cm
thickness which shields a set of detectors. The difference between the

shielded and unshielded detectors is therefore a measure of the thermal neutron fluence, while the shielded detectors measure the resonance fluence. The thickness of the ^{6}Li TLDs was 4.5 mg/cm^2 yielding a sensitivity of 0.0049 tracks/thermal neutron. The sensitivity for resonance neutrons (0.2 eV-1 MeV), where a $1/E_n$ spectrum is assumed, has been calculated to be 2.56 x 10^{-4} tracks/neutron. The thorium/mica detectors (when used) yielded a rough estimate of the high energy neutrons (> 1 MeV). The Th/mica recorded track densities contain both proton-induced and neutron-induced components (see Tables 12, 13, 14).
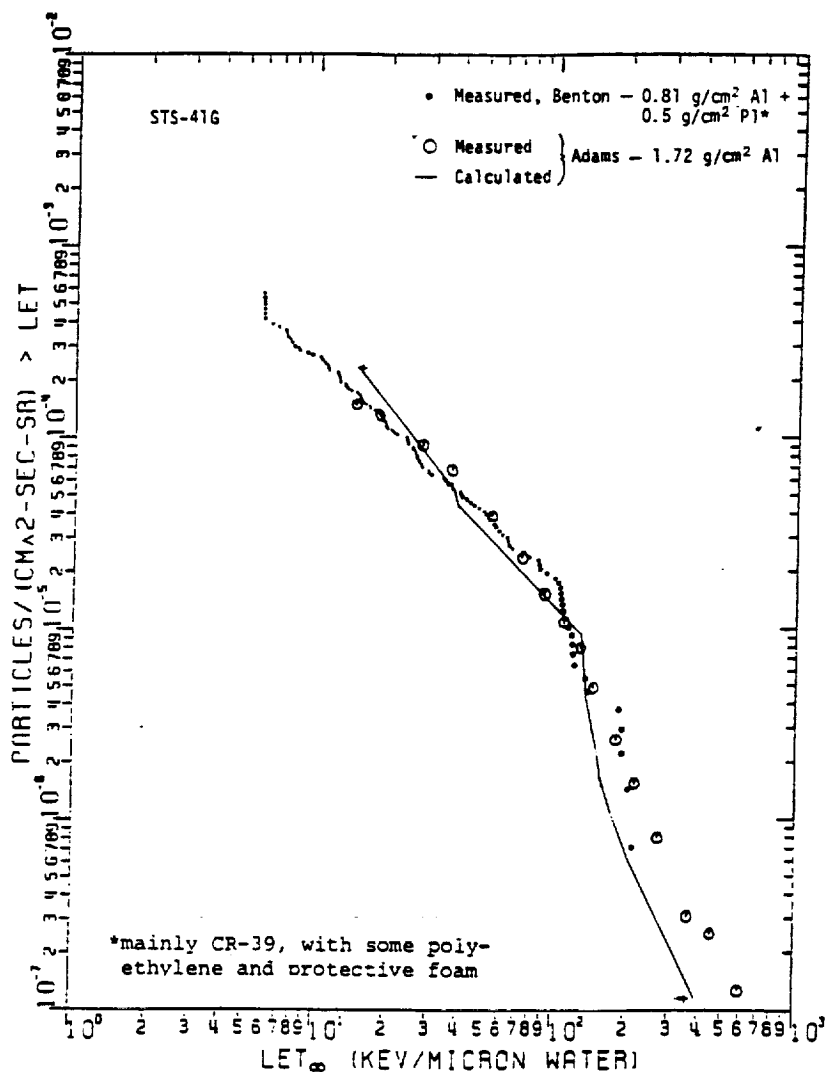

Fig. 20. Integral LET spectrum (total) for STS-41G, CRUX (experiment 3, No. 5-1, 2, batch USF3 /Adams, 1986; Benton, 1985/.

Table 12. Neutron Passive Detector Characteristics

Detector Type	Neutron Energy Range	Proton Energy Range
^{6}LiF/CR-39	0--1 MeV	--
Gd/^{6}LiF/CR-39/Gd	0.2 eV--1 MeV	--
^{238}U/mica	1.0 MeV	>15 MeV
^{232}Th/mica	1.2 MeV	>20 MeV
^{208}Bi/mica	>50.0 MeV	>50 MeV
^{181}Ta/mica	>1000.0 MeV	>1000 MeV

Detector Type	Sensitivity	Background
^{6}LiF/CR-39	$\left\{\begin{array}{l} 2.04 \times 10^2 \text{ thermal neutrons/track} \\ 3.90 \times 10^3 \text{ resonance neutrons/track} \end{array}\right.$	$\sim 150 \text{ cm}^{-1}$
Gd/^{6}LiF/CR-39/Gd		$\sim 100 \text{ cm}^{-1}$
^{238}U/mica	6.70×10^4 neutrons/track*	$\sim 0.5 \text{ cm}^{-1}$
^{232}Th/mica	1.38×10^5 neutrons/track*	$\sim 0.5 \text{ cm}^{-1}$
^{208}Bi/mica	1.44×10^6 neutrons/track*	$\sim 0.5 \text{ cm}^{-1}$
^{181}Ta/mica	$\sim 10^8$ neutrons/track*	$\sim 0.5 \text{ cm}^{-1}$

*Based on the neutron spectrum from Merker (Health Physics 25, 524-527, 1973). (for neutrons > 1 MeV).

Neutron Energy Range	QF	mrem-cm^2/neutron
<0.2 eV	2.0	1.02×10^{-6}
0.2 eV--1 MeV	6.4	4.92×10^{-5}
>1 MeV	10.0	5.95×10^{-5}

Neutron spectra have never been measured on spacecraft in orbit, while proton spectra are known only approximately for these flights. Therefore this method of measuring high-energy neutrons requires an assumption of a spectral shape in relative neutron-to-proton fluences based upon past space flight measurements and calculations of neutron production in the atmosphere. The fluence-to-dose conversion factors for thermal and resonant neutrons were from the NCRP /1971/; quality factors for thermal, epithermal and high-energy neutrons used were 2, 6.4, and 10 respectively. The accuracy of the thermal and epithermal neutron data is thought to be reasonable; however, the high energy neutron contribution which is bound to be of the most significance is fairly uncertain since the shape of the neutron energy spectra is not known.

7.0 STOPPING PARTICLES, SPALLATION PRODUCTS AND HIGH-LET RECOILS

A concern has existed for some time that short range, difficult to detect and measure, high LET tracks produced in tissue due to stopping protons, spallation products and proton-induced, high-LET recoils may have sig-

Table 13.   Neutron Measurements on Selected Space Missions

Energy Range and Flux Measurements $(cm^{-2}d^{-1})$

	< 1 MeV		> 1 MeV
Skylab	3.5×10^4		3.5×10^5

	0.02--2 eV		2 eV--2 keV
Apollo 11	$< 1.2 \times 10^6$		$< 4.0 \times 10^4$
Apollo 12	1.7×10^5		
Apollo 13	2.0×10^5		2.0×10^3

	< 0.3 eV	0.3 eV--1 MeV	> 1 MeV
Cosmos 936	2.0×10^4	6.6×10^4	1.1×10^5
Cosmos 1129	2.7×10^4	7.5×10^4	1.1×10^5

	< 0.2 eV	0.2 eV--1 MeV	> 1 MeV
STS-1	$< 2.2 \times 10^4$	$< 6.8 \times 10^4$	
STS-2	$< 7.8 \times 10^3$	$< 2.7 \times 10^4$	$< 1.6 \times 10^4$
STS-3	4.1×10^3	4.6×10^4	1.6×10^4
STS-4	6.1×10^3	4.7×10^4	3.4×10^4
STS-5	6.2×10^3	3.0×10^4	3.6×10^4
STS-6	6.0×10^3	7.6×10^4	2.2×10^4
STS-7	2.7×10^3	4.7×10^4	
STS-8	3.5×10^3	8.6×10^4	
STS-9	8.8×10^3	4.4×10^4	
STS-41B	2.4×10^3	1.4×10^4	
STS-41C	6.4×10^3	9.1×10^4	
STS-41D	1.0×10^3	5.1×10^4	
STS-41G	3.9×10^3	2.3×10^4	
STS-51A	5.0×10^3	2.4×10^4	

nificant radiobiological consequences. At least one biological phenomenon, that of light flashes observed by space crews, appears to be fluence dependent. The largest frequency of these events is observed during the passage through the SAA /Garriott, 1984; Savinykh, 1986/, as predicted by one of us /Benton and Henke, 1971/. Benton et al. /1972/ on Biosatellite III measured the high energy tail of the total recoil track distribution using plastic track detectors. Schaefer /1971, 1977, 1978/ using nuclear emulsions, measured the so-called "star" dose during the Apollo program. Space-based measurements of this component are difficult in that the measurement involves a track length distribution which ranges from the sub-micron region to a

Table 14.   Summary of Neutron Dose-Rate Data

Flight	Neutron Dose Rates (mrem/day)		
	Thermal	Resonance	High Energy
Cosmos 936	0.02	0.32	6.8
Cosmos 1129	0.03	0.40	6.8
STS-1	< 0.02	< 0.33	---
STS-2	< 0.01	< 0.13	1.0
STS-3	0.004	0.25	1.0
STS-4	0.006	0.23	2.0
STS-5	0.006	0.14	2.2
STS-6	0.006	0.38	1.3
STS-7	0.003	0.23	---
STS-8	0.003	0.43	---
STS-9	0.01	0.22	---
STS-41B	0.003	0.06	---
STS-41C	0.007	0.44	---
STS-41D	0.002	0.25	---
STS-41G	0.004	0.13	---
STS-51A	0.005	0.11	---

maximum of a few tens of microns while the detector may be in near satura-
tion due to primary particles.

The dose and dose-equivalent fraction of this component is significant
for lunar missions (see Table 15) /Schaefer, 1971/ and it is also expected
to be of importance for a space station type of orbit. The Biosatellite III
measurements yielded track density, ρ_R (Z >2, L_o >10 μm) $\cong 10^3$ cm^{-3}d^{-1}. This
number is expected to increase considerably once the shorter tracks are
taken into consideration.

Since the methods of measuring the charge and energy of all short-range
interaction products and recoil particles have limitations, evaluation of
the dose due to this component will depend more heavily on calculations.
Calculations have been made of the absorbed dose and dose-equivalent for
the secondary components from free space cosmic protons and for an SAA pro-
ton spectrum behind 20 g/cm^2 of aluminum /Armstrong, 1972; Santoro, 1972/.
The dose contribution from secondary heavy nuclei, protons, pions, leptons
and photons were individually calculated for depths up to 15 cm in tissue.
In the case of the GCR protons, after ~2 cm depth, the dose-equivalents due

Table 15.   Components of Mission Dose on First Lunar
             Landing Mission, Apollo XI

Component	Absorbed Dose, millirad	Dose Equivalent millirem
Protons	150	220
Stars	15	94
Fast neutrons	∿1	∿12
Heavy nuclei	5	46
Electrons and gamma rays	∿30	∿30
Total	201	402

/Schaefer, 1971/

to the secondary protons and secondary heavy nuclei both exceeded that due
to the primary ionization of incident protons (∿4 rem/yr from the secondary
heavy nuclei). On the other hand, for the trapped protons, the heavy nuclei
and secondary protons both contributed a dose-equivalent of ∿10% or more of
the primary ionization. These results depended heavily 1) on the QFs used
(a single Q = 20 for the heavy secondaries) and 2) on the intranuclear cas-
cade model used to obtain the distribution of the heavy target fragments/Ber-
tini, 1969; MECC7/. More recent experimental work using heavy energetic par-
ticle beams from accelerators has improved the knowledge of the distribution
of the mass and energy of the heavy target fragments. Relativistic beams of
carbon and oxygen were fragmented on a series of targets ranging from hydro-
gen through lead /Heckman, 1975; Greiner, 1975, Lindstrom, 1975/. The momen-
tum distribution of the multiply-charged projectile fragments were found to
be related to the Fermi motion of the fragments. The average fragment energy
as a function of the fragment mass was reasonably well represented by calcu-
lational models /Bertini, 1972/. However, the fragment production cross-
sections were significantly different from those of the Bertini models, as
shown in Table 16. As a result there is a large difference in the energy
transfer cross sections (also displayed in the table). Greater differences
will appear in the dose-equivalent because of the high QFs at high LET values
as shown in Fig. 21 /Wilson, 1977, 1987/. The integral LET spectra are for
single nuclear collisions of 2 GeV protons in water. Contributions from
alpha particles derived from the Bertini model are included. Although the
total event energy deposited differs by a factor of ∿35%, the highest LET

Table 16.* Comparison of Fragmentation Cross Sections (MBN) and Fragment Energy Transfer Cross Sections (MeV-MBN) of Bertini with experiments /Greiner et al., 1975/.

A_F	$\sigma_{BERTINI}$	$\sigma_{GREINER}$	$\overline{E}\sigma_{BERTINI}$	$\overline{E}\sigma_{GREINER}$
16	4.69	.02	5.04	.0006
15	103.4	61.5	60.6	56.9
14	40.0	35.4	48.8	51.7
13	18.5	22.8	37.6	48.3
12	32.2	34.1	85.8	68.2
11	8.2	26.4	37.9	99.1
10	11.0	12.7	52.8	62.0
9	1.2	5.2	6.5	25.7
8	.56	1.23	2.5	7.1
7	1.06	27.9	6.11	153.4
6	5.46	13.9	31.4	73.4
Total:	226.3	241.2	375.1	645.8

*Average integral energy transfer cross sections as a function of the LETs of heavy target products for a 2 GeV proton incident on water /Wilson, 1987/.
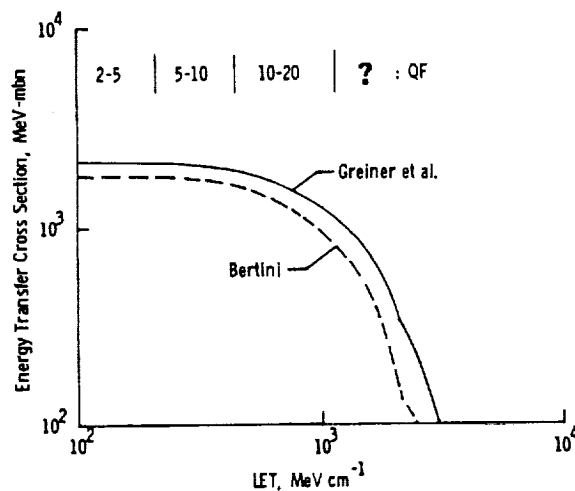

Fig. 21. Calculations from the Bertini model and derived from Greiner et al., 1975, are shown along with approximate quality factors for various LET regions /Wilson, 1987/.

components differ by a factor of three. Clearly, the assessment of risk from these components needs further work in measurement, calculation, and radiobiological studies.

8.0 INDUCED RADIOACTIVITY IN SPACECRAFT

Many materials, after exposure to high-energy space radiation, can become slightly radioactive. For gamma ray astronomers, this induced activity is of great concern since it makes a large and variable contribution to a gamma ray detector's background. This issue is of considerable interest for the Space Station since this will be a large spacecraft containing many types of materials and alloys, will spend many years in orbit, and will be bombarded by high fluxes of trapped protons (E > 30 MeV) as well as GCR, and high energy secondary neutrons (from the Earth's atmosphere or the spacecraft itself). Fishman /1974/ analyzed samples of various metals carried on Skylab 4 (400 km, 50^0, 84 d) at four locations with different shielding. The gamma ray activity from these samples was counted with high resolution germanium spectrometers after return to Earth. Counting began one week after sample return, and data was accumulated for $\sim 10^6$ s per sample. This method is not sensitive to very short half-life nuclides or those emitting short-range radiations (βs) but covers activity that significantly builds up in the spacecraft and deposits energy in the form of gamma rays in the crew areas. The data from the Skylab 4 samples, corrected to activity in orbit, and extrapolated to a very long exposure time (saturated activity) are shown in Table 17.

Following the re-entry of Skylab, some of the debris was found in Australia, returned to the U.S., and analyzed by Fishman and Meegan /1980/ (see Table 17). It should be noted that Skylab spent several months in low orbit below the SAA before re-entry so the shorter half-life nuclides in these results reflect the GCR and Earth albedo exposure only.

On the Apollo 17 mission and also on ASTP, Dyer et al. /1975/ and Trombka /19--/ flew NaI(Tl) scintillation crystals and made induced activity measurements with them immediately after return. The measurements indicated specific activation in ratio with the cosmic ray exposures of the two crystals and clearly showed activation lines due to neutrons.

Neutron measurements based on gamma ray line identification of specific nuclides with high neutron capture cross-sections have been made on a few occasions /Fishman, 1974; Keith, 1987/. They generally require long exposures to yield statistically significant results and the high energy measurements require complex corrections for proton interactions as do other passive techniques /Benton, 1985b/.

774

Table 17

17a). Specific Activities of Skylab-4 Activation*

Material-Interaction	Isotope	Half-Life	Specific Activity (Saturated)			
			1	2	3	4
$^{181}Ta + n$	^{182}Ta	115 d	17	7.9	5	3.9
$^{58}Ni + n$	^{58}Co	71 d	4.5	4.2	4.0	3.9
$^{58}Ni + p$	^{56}Co	77 d	2	2.2	3.1	4
$^{48}Ti + p$	^{48}V	16 d	0.8	1.8	1.5	3.7

*Activity is in disintegrations/kilogram-second
Location 1: in film vault
Location 2: adjacent to water tank
Location 3: on workshop wall, forward
Location 4: on workshop wall, aft
These were in descending order of shielding
Statistical errors varied from 15% to 60%

17b). Specific Activity in Skylab Debris Samples**

Material	Isotope	$T\frac{1}{2}$	Specific Activity (at re-entry)
Al	^{22}Na	2.6 yr	1.1
SS	^{58}Co	71 d	0.8
SS	^{54}Mn	303 d	3.0
SS	^{56}Co	77 d	1.5

**Activity was extrapolated to re-entry time and was in dis/kg-s.
/Fishman and Meegan, 1980/.

It is noted that the saturated activities from the Skylab data vary over the range ~1-20 dis/kg-s. These are in the range of, or lower than, in some common minerals, or even ^{40}K activity in the human body. If the average saturated activity were as high as 10 dis/kg-s, the total activity in a 5×10^5 kg spacecraft would be about 150 micro-Curies, spread over a few tens of meters. An assessment of the activity and resulting contribution to dose of a spacecraft with a correct materials list and distribution would be useful, but has not been done.

9.0 COMPARISON OF DOSE MEASUREMENTS WITH CALCULATIONS

The development of methods for the accurate prediction of dose and particle flux have been long-term goals in the field of space radiation protection. Over the past two decades, a large effort has gone into the development of these methods and techniques and in applying them to many spacecraft and missions. In addition to predictions for manned flights, much of this work was motivated by a concern about radiation effects on electronic circuits, computers, solar cells, photographic material, and other radiation-sensitive components and experiments. Here, we refer only to a few selected examples and briefly discuss some of the major features and limitations of the calculations reported in the literature. The state of the art in performing such calculations was previously described by Langley /1970/. Even earlier calculation methods were described and compared with space-flight measurements for some of the Gemini, Apollo and OV1-XX flights /Case, 1969; Janni, 1969b/. The trapped proton and electron spectra as a function of McIlwain parameters (B, L) were assembled by several groups (Vette, Thede, Reagan). Sector (vector) shielding of the Gemini and Apollo spacecraft was developed from engineering drawings and by measurements using gamma ray sources. Methods were developed by which protons, electrons and bremsstrahlung photons were transported through the sector shielding and doses calculated at interior points. Initial comparisons on Gemini and the OV spacecraft showed that the trapped environmental models needed improvement, since predicted and measured doses differed by a factor of three or more for some of the models and orbit locations /Schneider, 1969; Radke, 1969; Janni, 1969b/. However, as the models were improved with new data, the differences were reduced.

By the time of the Skylab missions, the environmental models had been revised and the methods of particle transport had been improved, e.g., Watts and Burrell /1971/, Wright and Burrell /1972/, and Hill /1973/. Good agreement was found between calculated doses and measured doses at five locations in the command module on Skylab 2, with calculated values only 10% to 40% above the measured values /Janni, 1976/. Other comparisons within the Skylab Workshop were also within that range /Hill, 1976/. Dose measurements using TLDs and comparisons with calculations were also made in the Shuttle crew area /Atwell et al., 1987/ and in the Spacelab module /Parnell et al., 1986/. The measurements were within about a factor of two or better of the calculated values with the calculated doses being generally higher than the measurement values.

Methods used to transport protons, electrons and their bremsstrahlung photons, and GCR nuclei through the shielding of the Shuttle plus Spacelab-1

776

have been previously described / Burrell, 1964; Watts and Burrell, 1971;
Wright and Burrell, 1972/. The proton transport code uses an approximation
to account for interaction losses and energy deposited by secondaries, and
this causes an overestimate of the actual absorbed dose. Calculated doses
from this method were compared to those from a Monte Carlo calculation that
included all interactions and secondaries /Alsmiller et al., 1972/. For
trapped proton spectra, the Monte Carlo calculation gives absorbed doses
10-15% smaller and dose-equivalents less than 5% smaller than the approxi-
mation method. The transport method for electrons and bremsstrahlung pho-
tons /Watts and Burrell, 1971/ gives doses within a few percent of the more
complex methods such as ETRAN.

The method used to transport cosmic ray nuclei also contains approxi-
mations in the treatment of interactions and cascade build-up, but the accu-
racy is ∿20% for prediction of absorbed dose for shielding thicknesses of
up to ∿20 g/cm^2. Recently new transport methods for cosmic ray nuclei have
been developed for calculating LET spectra within spacecraft /Heinrich,
1977/; Letaw and Adams, 1986; Letaw, 1986/. The Cosmic Ray Effect on Micro-
electronics (CREME) model /Adams, 1986/ considers loss by ionization and
interaction but does not consider heavy fragments or production of other
secondaries. Comparisons of measured and CREME model calculated LET spec-
tra made with PNTDs are shown in section 5.0 of this paper.

The major limitations in the accuracy of the present methods used to
calculate absorbed dose and particle fluxes inside spacecraft arise princi-
pally due to a lack of detailed knowledge of the primary environments (flux,
spectra, temporal and directional properties) and of spacecraft shielding
distributions. Both the trapped particles and the GCR (up to several GeV)
have temporal variations due to solar activity /Webber and Lockwood, 1981;
Marenny, 1987; Heckman et al., 1970, 1972/ that are only approximately
accounted for through the use of the solar maximum and minimum models. In
addition to the temporal variations there are directional characteristics,
particularly of the trapped particles /Watts, 1987/ that have not previously
been incorporated into the calculations. The currently used omnidirectional
environments may be satisfactory in the case of spinning or celestial point-
ing spacecraft, but are not appropriate for gravity gradient or velocity
vector stabilized spacecraft such as the LDEF and the Space Station. At
present, the knowledge of the environments is generally considered to be
accurate only to a factor of ∿2.

Accurate calculation of the dose-equivalent within orbiting spacecraft
will probably require more precise calculation of the contribution from sec-
ondary charged components than has previously been included in STS-mission-

type oriented calculations. Of concern here is the contribution from the evaporation and recoil particles resulting from interactions in the tissues, the spacecraft shielding and materials. Such calculations also involve the use of quality factors that are presently uncertain for the highly-charged, low-energy, high-LET particles. Although calculations including all relevant effects have not been applied to missions and complex shielding geometries, example calculations with spherical aluminum shielding and tissue targets have clearly shown the importance of these secondaries /Armstrong, 1972; Santoro, 1972/. Those calculations also include the neutral components (neutrons, pions, etc.,) and their effects, although they are not tabulated separately in the results.

10.0 SUMMARY AND CONCLUSIONS

During the last twenty-five years, dosimetry data has been slowly accumulating in the U.S. and Soviet manned space programs. The data covers almost all manned flights, and thus a variety of low Earth orbits (from $\sim$210 km to 500 km) and translunar flights. Data exists from flights of Vostok to Salyut 7 and Gemini to Spacelab, with their various complexities of shielding.

Passive dosimeters have yielded integral dose and mission average dose-rate information for low-Earth orbit ($\gtrsim$ 500 km, and inclinations $\gtrsim$ 65°). For the lowest altitudes and typical locations in the spacecraft the dose is dominated by the highly penetrating GCR contributing 5-10 mrad/day (depending on inclination), which is nearly independent of spacecraft shielding. Measurements have shown that for various locations in the Spacelab-1 module (STS-41A, 250 km, 57°) the trapped particles from the SAA contributed at most 40% and typically 15% or less of the total dose /Parnell et al., 1986/. At higher altitudes (350-500 km) the picture changes dramatically, with dose-rates increasing more than an order of magnitude and the bulk of the dose now coming from the trapped protons. Indeed, on mission STS-51J ($\sim$500 km, 28.5°), one passive dosimeter recorded an average mission dose-rate of nearly 200 mrad/day (arithmetic average shielding of $\sim$16.4 g/cm^2).

The complex shielding of the manned spacecraft causes variations in the dose as a function of location. The arithmetic average of shielding depth can be quite high (Cosmos 1129, $\sim$20 g/cm^2; Spacelab-1, 14-66 g/cm^2; Space Shuttle mid-deck, 16-30 g/cm^2). However, it has been shown that small solid angles (< 10% of 4π steradians) of thin shielding (< few g/cm^2) act as "radiation windows," causing dose to vary according to locations /Parnell et al., 1986; Atwell and Beever, 1987b/. These "thin windows" are not indicated in the arithmetic average of the shielding depth.

778

The number of locations that have been monitored limit the knowledge of the variation in dose due to shielding at different locations. Twenty-nine passive detectors showed a dose maximum/dose minimum variation of only 1.4 on Spacelab-1. On Skylab, five detectors showed a variation of 1.6, similar to the detectors on Salyut-7. The six detectors flown in the crew area of the STS at the highest orbit (51J) showed a ratio of 2.2. This indicates that the location dependency of dose rests largely on the trapped particle contribution, as expected. Most previous spacecraft have passed through the SAA in various attitudes, but the Space Station, which will have a somewhat similar attitude in the directional SAA flux, will be likely to have larger dose variations.

Only on several occasions have active detectors been used, tailored specifically to obtain data on space radiation dosimetry. Early measurements were made on Gemini and Apollo. Skylab carried a tissue-equivalent ion chamber and an LET spectrometer. On Cosmos 936 the Soviets flew an active LET spectrometer inside and outside the spacecraft /Kovalev et al., 1981/. On Spacelabs 1 and 2, Parnell et al. /1986/ and Fishman et al. 1986a/ employed active detectors which contributed significant information on the temporal variations of the radiation field inside the Spacelab module and on the pallet. These instruments allowed the separation of dose into its components of GCR, trapped protons and the bremsstrahlung from trapped electrons. Also, frequent occurrences of bremsstrahlung photon "bursts" were observed from electrons precipitating from the trapped belt. This work clearly showed the importance of detailed real-time dosimetry for the Shuttle flights, and particularly for the Space Station.

In the absence of detailed information on the flux, charge and energy spectra of charged particles, LET spectra have been measured on several missions. There is general agreement between the reported U.S. and Soviet results, even though the methods used (electronic detectors, nuclear emulsions, plastic track detectors) are different. The LET spectra clearly show differences between low and high inclination and altitude missions. However, relatively few missions, orbits, and shielding situations have been covered and much more data is needed.

While a reasonable amount of data exist for low altitude (< 500 km) and low inclination orbits, there is insufficient experimental dosimetric data for high altitude (> 500 km), polar, and geostationary orbits.

Very little data exist on the neutron component, but the measurements that have been made indicate it cannot be ignored on future missions, particularly in large spacecraft such as the Space Station. Neutron energy spec-

tral measurements need to be made as soon as possible, although this will be difficult to accomplish. There is no direct information available on the temporal variation of neutrons.

Since the LET spectra have not been measured on all missions and the neutron fluence has seldom been measured, a complete assessment of the dose-equivalent cannot be made. However we can give estimates of the fractions of dose-equivalent on a few missions. The fractions of low LET dose (from TLDs), high LET dose (from track detectors), and neutron dose (from fission foils) in the Spacelab-1 module (250 km, 57°) are approximately 30%, 56%, and 14%, respectively. On STS-5 (297 km, 28.5°) the fractions were ~54%, 27%, and 21%. High energy neutron measurements for higher altitude STS flights are not available for a similar comparison.

There have been some comparisons of dose and LET data with calculations that model the primary particle environments, the orbital parameters, and shielding distributions (usually simplified). Recent comparisons generally indicate that for total dose the predictions are too high. On Spacelab-1 the predictions were high by a factor of $\gtrsim 2$ /Parnell et al., 1986/. The calculations are based upon isotropic flux models, whereas the trapped environment is highly anisotropic /Heckman and Nakano, 1963/. This fact, and the effects of "thin windows" in shielding make such comparisons approximate at best. The trapped proton and electron environments have temporal changes which the models do not fully take into account, that may also affect the calculated doses and fluxes /Heckman and Lindstrom, 1972/. A comparison of LET measurements in a simple shielding situation (a GAS canister in the Space Shuttle bay) and a calculation based on GCR and geomagnetic effects agree quite well /Adams et al., 1986/. However, for situations involving greater amounts of shielding, the comparisons are not satisfactory /Letaw and Adams, 1986/. Such comparisons are also needed in more complex shielding situations and extending to low LETs where protons are important contributors of dose.

Several questions concerning temporal variations of dosimetric quantities can only be solved by long-term monitoring in various orbits. Solar activity affects both the trapped environment and the GCR flux. Higher solar activity heats and expands the Earth's atmosphere causing greater ionization loss of trapped particles and a decrease in flux in low Earth orbit. At the same time, the larger convected solar magnetic field "modulates" (reduces) the GCR flux at Earth. Very energetic, but rare, solar particle events can occasionally reach low Earth orbits. The effect of long-term secular variations in the geomagnetic field is also of concern.

It is important to determine the populations of short range tracks -- recoils and spallation products that arise as the result of irradiation of

780

tissue with cosmic ray nuclei and trapped energetic protons--and to assess their radiobiological consequences.

Finally, much more detailed information is needed on how the different components of the radiation field contribute to the overall dose and their spatial and temporal variations, as well as the effect of complex shielding distributions, before reasonably accurate extrapolations can be made to the case of the Space Station and other future missions of long duration.

The following is a partial summary of Soviet regulations, recently enacted, which deal with radiation safety of space crews and related issues.

APPENDIX

USSR STANDARDS FOR SPACE CREW RADIATION SAFETY IN SPACE FLIGHT

OUTLINE

	Type of Document and Effective Date	Title of Document
1.	Guiding Normative Document RD 50-25645.209-85 1 July 1987	SYSTEMATIC INSTRUCTIONS: SPACE CREW RADIATION SAFETY DURING SPACE FLIGHT (System for measuring cosmonauts' Individual dose during their career)
2.	USSR Government Standard GOST 25645.215-85 1 Jan. 1987 through 1 Jan. 1992	SPACE CREW RADIATION SAFETY DURING SPACE FLIGHT (Safety norms with flight duration up to three years)
3.	USSR Government Standard GOST 25645.202-83 1 Jan. 1986 to 1 Jan. 1992	SPACE CREW RADIATION SAFETY DURING SPACE FLIGHT (Requirements for individual and on-board dosimetric control)
4.	USSR State Committee of Standards. GOST 25645.214-85 1 Jan. 1987	SPACE CREW RADIATION SAFETY DURING SPACE FLIGHT (Model of generalized radiobiological effect)
5.	USSR Government Standard GOST 25645.203-83 1 Jan. 1985	SPACE CREW RADIATION SAFETY DURING SPACE FLIGHT (Model of human body for computation of tissue dose)
6.	Guiding Normative Document RD 50-25645.309-85 1 Jan. 1987	SYSTEMATIC INSTRUCTIONS: STANDARD METHODS OF EXPERIMENTAL DETERMINATION OF THE FUNCTION OF SHIELDING ELEMENTS AND TECHNICAL EQUIPMENT INSIDE A SPACECRAFT FROM IONIZED RADIATION
7.	USSR State Standard 25645.134-86 (no date given)	SOLAR COSMIC RAYS. A MODEL OF PROTON FLUXES

8. USSR Government Standard   SPACE CREW RADIATION SAFETY DURING SPACE
    GOST 25645.211-85   FLIGHT
    1 July 1987   (Nuclear interaction characteristics of
                                  protons)

9. USSR Government Standard   SPACE CREW RADIATION SAFETY DURING SPACE
    GOST 25645.212-85   FLIGHT
    1 Jan. 1987   (Nuclear interaction characteristics of
                                  multicharged ions)

10. USSR Government Standard   PENETRATION OF COSMIC RAYS INTO EARTH'S
    GOST 25645.116-84   MAGNETOSPHERE
    1 Jan. 1986   (Terms and definitions)

SUMMARIES OF DOCUMENTS

1. SYSTEMATIC INSTRUCTIONS
    SPACE CREW RADIATION SAFETY DURING SPACE FLIGHT
    (System for measuring cosmonauts' individual dose during their career:
    Guiding Normative Document RD 50-25645.209-85. Effective 1 July 1987.

    These instructions establish the system for measurement and control of
individual radiation doses received by cosmonauts from all types of radio-
active exposure during their career, and the system for determining the
doses received from radiological examinations. The instructions also imple-
ment control for observance of the norms of space crew radiation safety in
space flight. They apply to all authorities concerned with the selection,
training and medical examination of cosmonauts and to the USSR Ministry of
Health Radiation Safety Service which implements cosmonaut radiation safety
measures. The document states that radiological examination of cosmonauts
must be conducted on standard X-ray equipment, and that all X-ray radiation
received by cosmonauts in pre-acceptance examinations, periodic examination
at all stages of their careers, examination during cases of illness, and
during space flight is subject to obligatory measurement and control. The
procedure for examination at the first selection as cosmonaut candidates an
the periods for planned radiological examination of cosmonauts' organs is
outlined. The document lists the organs of the body which are subject to
count, assessment and control or radiation dose absorption, and gives a for
mula for this purpose. Tables show the values for specific dose strengths
for various areas of the body, including organs, joints, cavities, verte-
brae, etc.

    Requirements for collection, registration, storage and control of in-
formation concerning individual doses of radiation of cosmonauts are given
in detail. A general medical record is kept of all types of radiological
examinations conducted at all stages of the cosmonauts' preparation, but
individual radiation doses are recorded in a special chart which is the cos
monauts' basic document throughout their career. This chart is kept where-

ever the cosmonaut underwent the last medical examination. An example of
this chart and specific details of correct maintenance of the chart are
given. Protection against random duplication of radiological examination
by different medical personnel or in different institutions is provided by
this chart, which is controlled by a representative of the USSR Ministry of
Health Radiation Safety Service. The Ministry assesses the individual radi-
ation dose of the cosmonauts at any stage of their career and gives conclu-
sions to the medical commission upon demand.

2. SPACE CREW RADIATION SAFETY DURING SPACE FLIGHT
   (Safety norms with flight duration up to three years)
   USSR Government Standard GOST 25645.215-85. Effective 1 January 1987
   through 1 January 1992.

   Standards are established for space crew radiation safety norms during
space flights of up to three years' duration and for the period of the cos-
monaut's career. These standards are obligatory in all stages of develop-
ment of space crew radiation safety support systems, i.e., in development
of space flight programs and activities of crews; in planning of space crew
radiation protection and testing its effectiveness; in planning on-board
and individual dosimetric control and its implementation in space flight;
in the execution of planned projects and operational measures for implemen-
tation of radiation safety; in the planning of radiological examination of
cosmonauts. The radiation safety norms include: normative level of radia-
tion risk; maximum allowed dose-equivalent of radiation in the absence of
probable sources of radioactive danger; control of hourly average equiva-
lent dose; maximum allowed dose-equivalent of a single radiation exposure
during space flight; maximum allowed dose-equivalent during a cosmonaut's
career (not to exceed 4 Sv). The document gives methods of calculating the
above-mentioned safety norms, states the dose-equivalent of instant expo-
sure during a space flight (not to exceed 0.5 Sv), and gives methods of
determining values of dose-equivalent during a space flight and during a
cosmonaut's period of preparation, selection and medical examination. A
table giving the values of normalized quantities for flights of various
durations is provided and explanation of terms of reference is also given.

3. SPACE CREW RADIATION SAFETY DURING SPACE FLIGHT
   (Requirements for individual and on-board dosimetric control)
   USSR Government Standard GOST 25645.202-83. Effective 1 January 1986
   to 1 January 1992.

   Standards are established for individual and on-board dosimetric con-
trol requirements for manned space flights. Various categories of radia-
tion situations are defined by means of the ratios of the hourly dose-

equivalent to the control hourly dose-equivalent, giving the values of relative radiation risk. These ratios are given in a table showing ranges from "safe radiation" to "emergency radiation" situations. The choice of measures to ensure radiation safety of space crews is made with regard to the different radiation situation categories (RSCs) in which they may be placed, the main task of dosimetric control, therefore, being to assess the RSC and determine the generalized dose of radiation received by each crew member during flight. "Dosimetric control" is defined as a combination of individual and on-board dosimetric control (ODC); requirements for both types of control are specified as follows:

Individual dosimetric control. Methods include individual reading dosimeters, individual passive dosimeters, and ground or on-board testers to take readings from passive individual dosimeters. Must include absorption or dose-equivalent in case a radiation situation becomes non-standard, dangerous or emergency-status. (Note: a dose on the surface of a man's body is considered to be a dose at points where the depth is 7×10^{-5}m from the surface of the body.) The document states that individual passive dosimeters are intended for continuous wear by crew members throughout the flight; individual reading dosimeters need not always be worn in safe or standard RSCs but must then be placed in the compartment where crew members spend most of their time. Individual dosimeters must be capable of measuring radiation in all crews' work conditions, including extra-vehicular activity (EVA). The number and placement of individual and ODC systems must allow measurement of the generalized dose received by each crew member.

On-board dosimetric control. The ODC assesses the RSC and measures the generalized radiation dose by means of results of individual dosimetric control. To determine this dose, ODC must ensure reception of information necessary to calculate the quality of ionized radiation, space and time irregularities of the field of dose distribution, and measure the absorption and hourly dose-equivalent of radiation. To assess the RSC, the ODC must determine the generalized dose of radiation, and the correspondence of a radiation situation with its projected model, including information which establishes the source of ionized radiation which caused the degradation of the radiation situation. The ODC must also provide the crew with information concerning changes in the RSC. Information measured by the ODC must be transmitted to Earth via radio-telemetric system channel either by sampling or in complete form. The frequency and amount of information transmitted must be determined by the RSC. Technical work is performed by the dosimetric control system.

Under the heading "Volume and dosimetric control operation," the docu-

ment states that composition, volume and operation of dosimetric control is established in a technical system which ensures the radiation safety of spacecraft crews and requires expertise corresponding to the normative-technical document in force. The document enumerates further detailed requirements for dosimetric control:

a) Dosimetric control system composition and its volume must correspond to the requirements of these standards.

b) All crew members must be provided with individual dosimeters.

c) The dosimetric control system must be capable of changing its mode of operation, depending on the RSC.

d) During safe and standard radiation periods, the results of ODC must be available to the crew on demand.

e) During non-standard, dangerous or emergency radiation situations, the results of ODC must be available to the crew continuously, but for individual dosimetric control, reading dosimeters must be used.

f) During non-standard, dangerous or emergency situations, the results of individual dosimetric control must be entered into the information processing unit to determine the generalized radiation dose.

g) When a radiation situation shifts into a dangerous or emergency category, signals corresponding to the changes of the radiation situation must be given to the crew.

4. SPACE CREW RADIATION SAFETY DURING SPACEFLIGHT
· (Model of generalized radiobiological effect)
USSR State Committee of Standards GOST 25645.214-85. Effective 1 Jan. 1987.

This standard establishes a mathematical model of a generalized radiobiological effect depending on the time distribution of a radiation dose-equivalent. It is intended for determination of radiation risk when evaluating and providing for the radiation safety of a spacecraft crew during space flight as required by GOST 25645.215-85. The generalized radiobiological effect (GRE) is understood as the risk faced by the crew of a space vehicle during space flight when determined sources of radiation exposure are present and probable sources are absent. The document states that:

a) The GRE characterizes quantitatively an increase in the mortality rate as a result of somatic radiobiological effects, developing as a result of radiation exposure.

b) The model of the GRE consists of a model of the dependence of the GRE on the generalized dose of radiation (GDR) and a model of the dependence of the power of the radiation dose on the time distribution of the equivalent dose of radiation.

c) In the model of the dependence of the GRE on the GDR it is accepted that the GRE changes in proportion to the mortality rate in the absence of radiation exposure.

d) The dependence of the power of the GDR on the time distribution of the equivalent dose of radiation is accepted according to the model of effective dose, which reflects the rise and fall of radiation damage to the human organism in the time following radiation exposure.

Formulae are presented to represent the dependence of GRE on GDR, taking into account such factors as time, power of the GDR, age of the cosmonaut, etc.

5. SPACE CREW RADIATION SAFETY DURING SPACE FLIGHT
    (Model of human body for computation of tissue dose)
    USSR Government Standard GOST 25645.203-83. Effective 1 Jan. 1985.

Standards established for the form and basic dimensions of a model of a human body and coordinates of representative points for computation of tissue dose of cosmic radiation and the development of documentation during design of such models for conducting experimental research. The standards are binding for organizations occupied with determination of the spatial distribution of an ionized radiation field in a cosmonaut's body with regard to spacecraft crew radiation protection. The model used for this purpose is an anthropomorphic, tissue-equivalent, homogeneous figure having the form and average dimensions of a human male. Simplified models, cylindrical and spherical, will also be used.

Tables and figures with accompanying text present in detail the form, basic dimensions, representative points and chemical composition of all three models: anthropomorphic, cylindrical and spherical.

An anthropomorphic figure must be used to determine the characteristics of an ionized radiation field in a cosmonaut's body and to assess the error of determining these characteristics with the aid of an average model. A cylindrical model must be used to determine the characteristics of an ionized radiation field, necessary for calculation of the generalized dose, taking into account the irregularity of space radiation. A spherical model must be used for approximate assessment of a generalized dose. Using representative points in a real human (average male) as a guide, values of the equivalent dose in similar points on the models should be used in the calculation of the generalized dose in order to evaluate the effectiveness of radiation protection for the crew of a space vehicle.

6. SYSTEMATIC INSTRUCTIONS
    STANDARD METHODS OF EXPERIMENTAL DETERMINATION OF THE FUNCTION OF
    SHIELDING ELEMENTS AND TECHNICAL EQUIPMENT INSIDE A SPACECRAFT FROM
    IONIZED RADIATION
    Guiding Normative Document RD 50-25645.309-85. Effective 1 Jan. 1987.

Standard methods are established for determining functional shielding of elements (including technical equipment and crew members) inside spacecraft from ionized radiation. Tests are conducted on a model which must ensure the possibility of determining the mass surface current of controlled sections. This model must also include:

a) a coordinate system for moving the gamma radiation detector on cylindrical and/or spherical surfaces;

b) a point-wise isotropic single energy source of gamma radiation;

c) a gamma radiation detector;

d) an apparatus for registering the position of the source with respect to the detector and the number of impulses acting on the detector.

The method of measuring the functional screening of a point inside the object is described in detail, as are the basic parameters which characterize a source of non-dispersed gamma radiation and the measurements in a test process. A closed isotropic source of Cs 137 ($E_r = 661$ keV) with isotropy not exceeding ± 10% serves as a source of gamma radiation. A scintillating spectrometer with an inorganic NaI crystal and diameter equal to height serves as a gamma radiation detector. The creation of impulses corresponding to non-dispersed gamma radiation is done by means of amplitudinal impulse discrimination levels A_1 and A_2. Level A_1 corresponds to the maximum peak of photo-absorption and level A_2 is 20% less than level A_1. Formulae for determining the mass surface density and the impulse counting speed follow.

Tests are conducted in normal climactic conditions as defined by GOST 20.57.406-81 and duration of the test is determined by the number of points being measured for screening function. Personnel participating in the tests must have a third-class rating for safe operation of electrical installations with voltage loads up to 1000 volts. The work foreman must have an engineer-physicist rating.

Detailed instructions are given for graduated measurements of radiation by the amplitude distribution of pulses within the detector. The registered number of impulses for any control section must be no less than 4×10^3.

7. SOLAR COSMIC RAYS. A MODEL OF PROTON FLUXES
    USSR State Standard 25645.134-86. No effective date given.

This document establishes a model of proton fluxes of solar cosmic rays (SCR) with energy $E \geq 10$ MeV in interplanetary space beyond the magnetosphere of the Earth near the plane of the ecliptic at a distance of approximately one astronomical unit from the sun in different periods of the 11-year cycle of solar activity. The standard is intended for use in calcula-

tions of the radiation activity of SCR fluence on technical devices, biological and other objects in outer space. The duration and position of the beginning of the 11-year solar activity cycle are determined from GOST 25645. 302-83. The present document gives formulae for calculating the duration of active and passive periods (characterized by different values of SCR fluxes). The document states that, during passive periods of the 11-year cycle, a total fluence of protons of solar cosmic rays with energy $E \geq 10$ MeV is assumed equal to 10^7 cm^{-2}, regardless of the duration of the spaceflight. During the active period of the cycle, the total fluence of protons of solar origin, N_E cm^{-2}, for all proton energies greater than E, is a random quantity. This randomness is a result of the occurrence, during the flight period, of a random number of solar proton events. Equations are given to determine the distribution density of the total fluence of protons. Tables show the probabilities of exceeding the total fluence of protons for flights of duration varying from ten days to three years.

8.   SPACE CREW RADIATION SAFETY DURING SPACE FLIGHT
      (Nuclear interaction characteristics of protons)
      USSR Government Standard GOST 25645.211-85. Effective 1 July 1987.

    This document establishes the nuclear interaction characteristics of cosmic ray protons, as well as protons and neutrons (nucleons) formed by them in spacecraft shielding (secondaries), for the nuclei of elements from carbon to lead in the 20-1000 MeV nucleon energy range. Among the characteristics taken into consideration are the nucleon mean path to nuclear interaction and the double differential of energy and the exit angle of distribution of secondary nucleons in an inelastic nucleon-nucleus interaction. The methods and formulae for the calculation of the nuclear mean free path are given.

9.   SPACE CREW RADIATION SAFETY DURING SPACE FLIGHT
      (Nuclear interaction characteristics of multicharged ions)
      USSR Government Standard GOST 25645.212-85. Effective 1 January 1987.

    This document establishes standards of quantitative characteristics for the nuclear interaction of cosmic ray multicharged ions where the nuclear charge is from 2 to 29 units of the absolute value of the electron charge and the range of kinetic energy on a nucleon is from 10^2 to 10^4 MeV in tissue equivalent material and shielding materials. The document states that the

mean free path to nuclear interaction is related to nuclear interaction characteristics and the GCR nuclei fragmentation parameters. The values of the interaction path and fragmentation parameters are established for representative nuclei groups of GCR nuclei. For the other nuclei of the particular group of GCR nuclei, the characteristics of the nuclear interaction are taken as being the same as for the representative nucleus of that group.

Groups of GCR nuclei are specified in accordance with GOST 25645.104.84. Representative groups of nuclei are defined as follows: helium nuclei, light nuclei, medium nuclei, heavy nuclei and very heavy nuclei groups. Nuclear fragments which form as a result of nuclear interaction are assembled in group J which is designated the same as for projectile nuclei with the addition of the group of protons with $Z = 1$, taking hydrogen ^1H as the representative nucleus. Composition of the tissue-equivalent material is according to GOST 18622-79. Nuclear interaction characteristics are considered independent of the GCR nuclei kinetic energy for the energy interval under consideration.

Values of interaction paths of representative nuclei from each group of GCR nuclei in a fabric-equivalent medium, graphite, aluminum and iron are presented in a table. Values of interaction paths for other safety materials are defined in accordance with the recommendations in an appendix. Values of fragmentation parameters for representative nuclei groups of GCR in tissue are presented in a second table. Values of fragmentation parameters for representative nuclei groups of GCR with mass numbers ranging from 12 to 72 are presented in a third table.

10. PENETRATION OF COSMIC RAYS INTO EARTH'S MAGNETOSPHERE
    (Terms and definitions)
    USSR Government Standard GOST 25645.116-84. Effective 1 January 1986.

This document establishes terms and definitions to be used in science and engineering with reference to the penetration of cosmic rays into the Earth's magnetosphere. These terms are obligatory for use in documents of all types, scientific-technical, educational and reference literature. One standardized term is established for each concept; synonyms may not be used. Short forms for distinct standardized terms are given as a reference. These may be used when there is no possibility of incorrect interpretation. In the standard, alphabetical indexes containing terms in Russian and their equivalent in English are given.

NOTES

1. Recommendations of the ICRU, 1970, ICRU Report No. 16 (II), Washington, D.C.
2. Digital Data Dosimetry, Tulsa, OK, Model 1/E-1.
3. Reuter Stokes, Cleveland, OH, Model RS-P3-0803-287.

ACKNOWLEDGEMENTS

REFERENCES

Adams, J. H., Jr., Tylka, A. J., and Stiller, B., 1986, LET spectra in low Earth orbit, IEEE Trans. Nucl. Sci., NS-333: 1386.

Akopova, A. B., Vikhrov, A. I., Dudkin, V. E., Magradze, N. V., Moiseenko, A. A. and others, 1985, Measurement of the spectrum of linear energy losses of cosmic rays by the Cosmos-1129 satellite, Cosmic Res. (ISSN 0023-4206) 23:479, in Russian.

Akatov, Y. A., Arkhangelsky, V. V., Aleksandrov, A. P., Fehér, I., Deme, S., Szabó, B., Vágyölgyi, J., Szabó, P. P., Csöke, A., Ránky, M., and Farkas, B., 1984, Thermoluminescent dose measurements on board Salyut-type orbital stations, Adv. Space Res., 4 (10):77.

Alsmiller, R. G., Santoro, R. T., Barish, J., and Clayborn, H. C., 1972, Shielding of manned vehicles against protons and alpha particles, ORNL Report RSIC-35.

Armstrong, T. W., Alsmiller, R. G., and Chandler, K. C., 1972, Monte Carlo calculations of high energy nucleon-meson cascades and applications to galactic cosmic-ray transport, Proceedings of the National Symposium on Natural and Man-Made Radiation in Space, NASA TM X-2440:117.

Armstrong, T. W., Chandler, K. C., and Barish, J., 1973, Calculations of neutron flux spectra induced in the Earth's atmosphere by galactic cosmic rays, J. Geophys. Res., 78:2715.

Atwell, W., Hardy, A. C., Beever, E. R., Richmond, R. G., and Cash, B. L., 1987a, A comparison of space radiation dose calculations with onboard dosimeter measurements for space shuttle missions, Oral presentation at Lawrence Berkeley Laboratory/DOE/NASA Workshop, "High Energy Accelerator and Space Radiation," Berkeley, CA, February 17-19, 1987.

Atwell, W., and Beever, E. R., 1987b, Space radiation exposures for manned polar missions: a parametric study, Proc. NATO Advanced Study Institute, Corfu, Greece, Oct. 11-25, 1987.

Bailey, J. V., 1977, Dosimetry during space missions, IEEE Trans. Nucl. Sci., NS-23 (4):1379.

Benton, E. V., and Collver, M. M., 1967, Registration of heavy ions during the flight of Gemini VI, Hlth. Phys., 13:495-500.

Benton, E. V., and Henke, R. P., 1971, High-Z particle Apollo astronaut dosimetry with plastics, Presented at the National Symposium on Natural and Man-Made Radiation in Space, Las Vegas, Nevada, March 1971.

Benton, E. V., Curtis, S. B., Henke, R. P., and Tobias, C. A., 1972, Comparison of measured and calculated high-LET nuclear recoil particle exposure on Biosatellite III, Hlth. Phys., 23:149.

Benton, E. V., Henke, R. P., and Bailey, J. V., 1975a, Heavy cosmic ray exposure of Apollo astronauts, Science, 187:263.

Benton, E. V., Henke, R. P., Peterson, D. D., Bailey, J. V., and Tobias, C. A., 1975b, High-LET particles in manned spaceflight--preliminary report, in: "Radiation Research," Academic Press, N.Y.

Benton, E. V., Peterson, D. D., Bailey, J. V. and Parnell, T. A., 1977, High-LET particle exposure of Skylab astronauts, Hlth. Phys., 32:15.

Benton, E. V., Henke, R. P., Frank, A. L., Johnson, C. S., Tran, M. T., and Etter, E., 1981, Space Radiation Dosimetry Aboard Cosmos 1129--Experiment K-309, USF-TR-53, University of San Francisco.

Benton, E. V., 1983, Dosimetric radiation measurements in space, Nucl. Tracks Rad. Meas., 7 (1/2):1.

Benton, E. V., 1985a, Unpublished work.

Benton, E. V., Frank, A. L., Henke, R. P., Rowe, V., and Atallah, T., 1985b, STS-51C dosimetry report, University of San Francisco, USF-TR-68.

Benton, E. V., 1986, Summary of radiation dosimetry results on U.S. and Soviet manned spacecraft, Adv. Space Res., 6 (11):315.

Benton, E. V., 1987, Cosmos 1887 (work in progress).

Bertini, H. W., 1969, Phys. Rev., 88:1711.

Bertini, H. W., Guthrie, M. P., and A. H. Culkowski, 1972, Nonelastic interactions of nucleons and π-mesons with complex nuclei at energies below 3 GeV, Oak Ridge National Laboratory ORNL-TM-3148, Oak Ridge, TN.

Bertini, H. W., MECC7, a Monte Carlo intranuclear cascade and evaporation code, Oak Ridge National Laboratory, Radiation Shielding Information Center, Oak Ridge, TN.

Bhatt, V. L., 1986, Neutron high-energy spectra at 5.mbar near the geomagnetic equator, J. Geophys. Res., 81 (25):4603.

Bücker, H., 1975, Biostack--a study of the biological effects of HZE galactic cosmic radiation, in: "Biomedical Results of Apollo," R. Johnston, L. Dietlein, M.D., and C. Berry, M.D., eds., NASA SP-368, Ch. 2, NASA, Washington, D.C.

Burrell, M. O., 1964, The calculation of proton penetration and dose rates, NASA TM-X-53063.

Case, R., 1969, Techniques used for the calculation of space radiation doses, Aerosp. Med., 40:1455.

Cervini, J. T., 1971, A summary of the OV1-19 measurements, Proc. Nat. Symp. Natural and Man-Made Radiations in Space, NASA TM-X-2440: 561.

Chan, K. W., Teague, M. J., and Vette, J. I., 1976, AE-6, a model environment of trapped electrons for solar maximum, NASA/GSFC report NSSDC-76-04.

Chan, K. W., Teague, M. J., and Vette, J. I., 1977, An interim outer zone electron model AE 1-7, NASA/GSFC report WDC-A-R-S 77-05.

Curtis, S. B., and Benton, E. V., 1980, Abundances, energy, and LET spectra of HZE particles in space, LBL-TR-11220, Lawrence Berkeley Laboratory.

Dudkin, V. E., 1987, private communication.

Dyer, C. S., Trombka, J. I., Schmadeback, R. L., Eller, E., Bielefeld, M. J., O'Kelley, G., Eldridge, J., Northcutt, K., Metzger, A., Reedy, R., Schonfeld, E., Seltzer, S., Arnold, J., and Peterson, L., 1975, Space Science Instrumentation, D. Reidel Co., Dordrecht, Holland, p. 279.

Fishman, G. J., 1974, Neutron and proton activation measurements from Skylab, AIAA Paper No 74-1227, presented at the AIAA/AGU Conference on Scientific Experiments of Skylab, Huntsville, AL, Oct. 30 to Nov. 1, 1974.

Fishman, G. J., and Meegan, C. A., 1980, Induced radioactivity in recovered Skylab materials, NASA TM-78263, NASA/Marshall Space Flight Center, AL.

Fishman, G. J., Paciesas, W. S., Meegan, C. A., and Wilson, R. B., 1986a, Gamma ray and charged particle background measurements in Spacelab-2, Adv. Space Res., 6, (4):23.

Fishman, G. J., Paciesas, W. S., and Gregory, J. C., 1986b, Measurements of background gamma radiation on Spacelab-2, Proc. XXVI COSPAR Meeting, Toulouse, June 30-July 12.

Frank, A. L., and Benton, E. V., 1987, Unpublished results.

Garriott, O. K., 1984, (U.S. astronaut), private communication on Skylab and Spacelab experience.

Greiner, D. E., Lindstrom, P. J., Heckman, H. H., Cork, B., and Bieser, F. S., 1975, Momentum distributions of isotopes produced by relativistic ^{12}C and ^{16}O projectiles, Phys. Rev. Lett. 35:152.

Haymaker, W., Look, B. C., Benton, E. V., and Simmonds, R. C., 1975, The Apollo 17 pocket mouse experiment (Biocore), in: "Biomedical Results of Apollo," R. S. Johnston, L. F. Dietlein and C. A. Berry, eds., U.S. Govt. Printing Office, Washington, D.C. (NASA-SP-368).

Heckman, H. H., and Nakano, G. H., 1963, East-west asymmetry in the flux of mirroring geomagnetically trapped protons, J. Geophys. Res., 68 (3)2117.

Heckman, H. H., Lindstrom, P. J., and Nakano, G. H., 1970, Long term behavior of energetic inner belt protons, NASA SP-3024.

Heckman, H. H., and Lindstrom, P. J., 1972, Response of trapped particles to a collapsing dipole field, J. Geophys. Res., 77 (4):740.

Heckman, H. H., 1975, Heavy ion fragmentation experiment at the Bevatron, NASA CR-142589, Washington, D.C.

Heinrich, W., 1977, Calculation of LET spectra of heavy cosmic ray nuclei at various absorber depths, Rad. Eff., 34:143.

Henke, R.P., and Benton, E. V., 1974, Heavy cosmic-ray measurements on Apollo 16 and 17 missions--results of the HZE dosimeter experiment, University of San Francisco, USF-TR-34.

Hill, C. W., 1973, Methods of treating complex space vehicle geometry for charged-particle radiation transport, Science Applications Inc. Report SAI-74-549-Hu.

Hill, C. W., 1976, Skylab post-mission radiation analysis, Science Applications Inc. Report 77-681-Hu.

Imhof, W. L., Reagan, J. B., Nakano, G. H., and Gaines, E. E., 1979, J. Geophys. Res., 84:6371.

Imhof, W. L., Voss, H. D., Walt, M., Gaines, E. E., Mobilia, J., Datlowe, P. T., and Reagan, J. B., 1986, Slot region electron precipitation by lightning, VLF Chorus, plasmospheric hiss, J. Geophys. Res., 91 (8): 8883.

Janni, J., 1969a, A review of Soviet manned space flight dosimetry results, Aerosp. Med., 40:1547.

Janni, J., 1969b, Spacecraft cabin radiation distributions for the fourth and sixth Gemini flights, Aerosp. Med., 40 (12):1527.

Janni, J., 1969c, Editor, Aerosp. Med., 40.

Janni, J., 1976, Skylab II--radiation dosimetry systems and flight results, Air Force Weapons Laboratory (Kirtland AFB) Report, AFWL-TR-73-222, NTIS No. AD-A032-409.

Keith, W., 1987, Private communication.

Kovalev, E. E., Benton, E. V., and Marenny, A. M., 1981, Measurement of LET spectra aboard Cosmos 936 biological satellite, Rad. Prot. Dos., 1 (3):169.

Langley, R. W., 1970, Space radiation protection, NASA SP-8054.

Letaw, J. R., and Adams, J. H., Jr., 1986, Comparison of CREME model LET spectra with spaceflight dosimetry data, SCC Report 86-01, Severn Communications Corporation.

Lindstrom, P. J., Greiner, D. E., Heckman, H. H., Cork, B., and Bieser, F. S., 1975, Isotope production cross sections from the fragmentation of ^{16}O and ^{12}C at relativistic energies, Lawrence Berkeley Laboratory, LBL-3650.

Lockwood, J. A., Chen, C., Friling, L. A., and St. Onge, R. N., 1986, Energy spectrum and flux of high energy neutrons at balloon altitudes, J. Geophys. Res., 81 (34):6711.

Marenny, A. M., Nymmik, R. A., and Saslov, A. A., 1987, Solar modulation of the galactic cosmic ray fluxes of heavy nuclei in 1974-1986, International Cosmic Ray Conference, Moscow, 1987, V. 3:328.

Markelov, V. V., and Chernykh, I. V., 1982, Direct-reading dosimeters used for monitoring radiation in Salyut stations, Kosmich. Biolog. Aviakosm. Meditsina, 16:81.

Mullen, E. G., Grussenhoven, M. S., and Hardy, D. A., 1987, The space radiation environment at 840 km, presented at NATO Advanced Study Institute, Corfu, Greece, Oct. 11-25, 1987.

Osborne, W. Z, and Pinsky, L. S., 1975, Apollo light flash investigations, in: "Biomedical Results of Apollo," R. Johnston, L. Dietlein, M.D., and C. Berry, M.D., eds., NASA SP-368, Ch. 2, NASA, Washington, D.C.

Parnell, T.A., Watts, J. W., Jr., Fishman, G. J., Benton, E. V., Frank, A. L., and Gregory, J. C., 1986, The measured radiation environment within Spacelabs 1 and 2 and comparison with predictions, Adv. Space. Res., 6 (12):125.

Peterson, D. D., and Benton, E. V., 1975, High-LET particle radiation inside Skylab (SL-2) command module, Hlth. Phys., 29:125.

Petrov, V., Akatov, Y., Kozlova, S., Markelov, V., Nesterov, V., Redko, V., Smirenny, L., Khortsev, A., and Chernykh, I., 1975, The study of the radiation environment in near-Earth space, Space Res., 13:129.

Radke, G., 1969, An evaluation of current methods of predicting space radiation doses by comparing calculations with Gemini IV OV1-2, OV1-4, and OV1-9 experimental measurements, Aerosp. Med., 40:1557.

Richmond, R. G., 1969, A review of Gemini and Apollo astronaut dosimetry data, Aerosp. Med., 40 (12):1535.

Santoro, R. T., Claiborne, H. C., and Alsmiller, R. G., Jr., 1972, Primary and secondary particle contributions to the depth dose distribution in a phantom shielded from solar-flare and Van Allen protons, Proc. Nat. Symp. Natural and Man-Made Radiation in Space, NASA TM X-2440, 117.

Savinykh, V., 1986, (Soviet cosmonaut), private communication.

Sawyer, D. M., and Vette, J. I., 1976, AP8 trapped proton environment for solar minimum and solar maximum, NASA/GSFC Report WDC-A-R&S, 76-06.

Schaefer, H. J., 1971, Apollo mission experience, Proc. Nat. Symp. Natural and Man-Made Radiation in Space, E. A. Warman, ed., NASA TM X-2440, NASA, Washington, D.C. (1972).

Schaefer, H. J., 1977, Nuclear emulsion measurements of the dose contribution from tissue-disintegration stars on the Apollo-Soyuz mission, ONR Contract No. 00014-76-C-0544, Report 2, Physics Department, Univ. of West Florida, Pensacola, FL 32504.

793

Schaefer, H. J., 1978, A note on the tissue star dose in personnel radiation monitoring in Space, NASA Contract No. NAS9-15417, Physics Dept., Univ. of West Florida, Pensacola, FL 32504.

Schneider, M. R., and Janni, J. F., 1965, Experiment D-8, radiation in spacecraft Gemini-4, in: "First Manned Spaceflight Symposium," Washington, D.C., p. 171.

Schneider, M. R., and Janni, J. F., 1969, A comprehensive summary of dose-rate measurements aboard the fourth and sixth Gemini flights, Aerosp. Med., 40 (12):1535.

Singley, G. W., and Vette, J. I., 1972, A model environment for outer zone electrons, NASA/GSFC Report NSSDC 72-13.

Stassinopoulis, E. G., 1987, Radiation environment in space, Presented at NATO Advanced Study Institute, Corfu, Greece, Oct. 11-25, 1987.

Teague, M. J., and Vette, J. I., 1974, A model of the electron environment for solar minimum, NASA/GSFC Report NSSDC-74-03.

Thede, A., 1969, OV3-4 dose rate and proton spectral measurements, AFWL-TR-68-128 (Kirtland AFB).

Trombka, J. I., Eller, E. L., Schmadebeck, R. L., Dyer, C. S., Reedy, R. C., Barr, D., Gilmore, J., Prestwood R., Bayhurst, B., Perry, D., Smith, A., Cordi, R., Pehl, R., Eldridge, J., Schonfeld, E., and Metzger, A., 19--, Crystal Activation Experiment MA-151, ASTP Summary Science Report, NASA-HQ report, unpublished.

Vette, J. I., 1966, Models of the trapped radiation environment, NASA-SP 3024, Vols. 1 and 2.

Vette, J. I., and Chen, C. K., 1987, Trapped electron environment models for solar minimum and solar maximum, available from NASA/GSFC-NSSDC, (private communication).

Vorobyov, Y. I., and Kovalyov, Y. Y., 1983, "Radiation Safety of Crews of Flying Vehicles," Energoatomizdat, Moscow, Ch. 7.

Watts, J. W., Jr., and Burrell, M. O., 1971, Electron and bremsstrahlung penetration and dose rates, NASA TN D-6385.

Watts, J. W., Jr., and Wright, J. J., 1976, NASA TM X-73358.

Watts, J. W., Jr., Parnell, T. A., and Heckman, H. H., 1987, An approximate angular distribution for trapped protons at low altitudes, Proceedings CHERBS, Sanibel Island, FL, Nov. 3-5, 1987.

Webber, W. R., and Lockwood, J. A., 1981, A study of the long-term variation and radial gradient of cosmic rays out to 23 AU, J. Geophys. Res., 36:11, 458.

Wilson, J. W., 1977, Analysis of the theory of high-energy ion transport, NASA TN D-8381.

Wilson, J. W., 1987, Private communication.

Wright, J. J., and Burrell, M. O., 1972, The estimation of galactic cosmic-ray penetration and dose rates, NASA TN D-6600.